U.S.N.A. --- Trident Scholar project report; no. 287 (2001)

Determination of Atmospheric Density in Low-Earth Orbit Using GPS Data

by

Midshipman John L. Young III, Class of 2001
United States Naval Academy
Annapolis, Maryland

_____

_____
Date

Certification of Adviser Approval

Professor Daryl G. Boden
Aerospace Engineering Department

_____

_____
Date

Acceptance for the Trident Scholar Committee

Professor Joyce E. Shade
Chair, Trident Scholar Committee

_____

_____
Date

Form SF298 Citation Data

Report Date *("DD MON YYYY")* 07052001	**Report Type** N/A	**Dates Covered (from... to)** *("DD MON YYYY")*

Title and Subtitle Determination of atmospheric density in low-earth orbit using GPS data	**Contract or Grant Number**
	Program Element Number
Authors Young, John L.	**Project Number**
	Task Number
	Work Unit Number
Performing Organization Name(s) and Address(es) US Naval Academy Annapolis, MD 21402	**Performing Organization Number(s)**
Sponsoring/Monitoring Agency Name(s) and Address(es)	**Monitoring Agency Acronym**
	Monitoring Agency Report Number(s)
Distribution/Availability Statement Approved for public release, distribution unlimited	
Supplementary Notes	
Abstract	
Subject Terms	
Document Classification unclassified	**Classification of SF298** unclassified
Classification of Abstract unclassified	**Limitation of Abstract** unlimited
Number of Pages 89	

REPORT DOCUMENTATION PAGE

Form Approved
OMB No. 074-0188

1. AGENCY USE ONLY (Leave blank)	2. REPORT DATE	3. REPORT TYPE AND DATE COVERED
	7 May 2001	

4. TITLE AND SUBTITLE
Determination of atmospheric density in low-earth orbit using GPS data

5. FUNDING NUMBERS

6. AUTHOR(S)
Young, John L.

7. PERFORMING ORGANIZATION NAME(S) AND ADDRESS(ES)

8. PERFORMING ORGANIZATION REPORT NUMBER

9. SPONSORING/MONITORING AGENCY NAME(S) AND ADDRESS(ES)
US Naval Academy
Annapolis, MD 21402

10. SPONSORING/MONITORING AGENCY REPORT NUMBER
Trident Scholar project report no. 287 (2001)

11. SUPPLEMENTARY NOTES

12a. DISTRIBUTION/AVAILABILITY STATEMENT
This document has been approved for public release; its distribution is UNLIMITED.

12b. DISTRIBUTION CODE

13. ABSTRACT:
The objective of this project was to develop an algorithm to accurately determine atmospheric density using simulated GPS data. This algorithm is designed to support a future USNA Small Satellite mission. Atmospheric density is the most variable factor in orbit propagation. Thus, the uncertainty in density generates the most error when predicting a satellite=s future position. Numerous models have been developed to account for the variations, but more accurate models are needed. In developing the algorithm, Satellite Tool Kit (STK), Analytical Graphics Inc.=s orbit propagation software, was used to generate data using one of several atmospheric models. By measuring the changes in the satellite=s orbit due to atmospheric drag, the density was accurately calculated to within 1% of the 1976 Standard Atmospheric Model. To validate the algorithm, the density output was compared to that of the model used in STK. The USNA Small Satellite Program has planned to design and place a satellite in low-Earth orbit (LEO) with a GPS receiver on board. The primary mission of the satellite is to determine density in the upper atmosphere. Once the USNA satellite is on orbit, the algorithm can be used to create a database of densities. Other small satellite programs will launch similar satellites to generate sufficient data. With the new atmospheric density data, scientists can create an improved atmospheric model.

14. SUBJECT TERMS
atmospheric density; atmospheric density models; GPS; small satellites; atmospheric drag

15. NUMBER OF PAGES
96

16. PRICE CODE

17. SECURITY CLASSIFICATION OF REPORT	18. SECURITY CLASSIFICATION OF THIS PAGE	19. SECURITY CLASSIFICATION OF ABSTRACT	20. LIMITATION OF ABSTRACT

Abstract

The objective of this project was to develop an algorithm to accurately determine atmospheric density using simulated GPS data. This algorithm is designed to support a future USNA Small Satellite mission. Atmospheric density is the most variable factor in orbit propagation. Thus, the uncertainty in density generates the most error when predicting a satellite's future position. Numerous models have been developed to account for the variations, but more accurate models are needed.

In developing the algorithm, Satellite Tool Kit® (STK), Analytical Graphics Inc.'s orbit propagation software, was used to generate data using one of several atmospheric models. By measuring the changes in the satellite's orbit due to atmospheric drag, the density was accurately calculated to within 1% of the 1976 Standard Atmosphere Model. To validate the algorithm, the density output was compared to that of the model used in STK®.

The USNA Small Satellite Program has planned to design and place a satellite in low-Earth orbit (LEO) with a GPS receiver on board. The primary mission of the satellite is to determine density in the upper atmosphere. Once the USNA satellite is on orbit, the algorithm can be used to create a database of densities. Other small satellite programs will launch similar satellites to generate sufficient data. With the new atmospheric density data, scientists can create an improved atmospheric model.

Keywords:

Atmospheric Density
Atmospheric Density Models
GPS
Small Satellites
Atmospheric Drag

Acknowledgements

I would like to thank Professor Boden for his support throughout this project. Without his assistance and input, this project would not have been possible.

Table of Contents

List of Tables

List of Figures

List of Symbols

A: Cross sectional area
$\vec{a}$: Acceleration
a: Semimajor axis
C_D: Coefficient of drag
e: Eccentricity
H: Scale height
h: Height
m: Mass
n: Mean motion
r: Position
v: Velocity

ϕ_{FPA}: Flight Path Angle
ϕ_{SAT}: Satellite's Latitude
μ: Earth's gravitational parameter
ρ: Atmospheric density
n: True Anomaly
ξ: Specific Mechanical Energy
$\Omega_{\oplus}$: Angular Rotation of the Earth

Introduction

Density variations in the upper atmosphere are common and current density models can deviate from realistic conditions. However, with sufficient data, scientists can develop newer, more accurate models. By using a Global Positioning System (GPS) receiver on board a satellite, one can obtain data in the form of time, position, and velocity. With these data, it is possible to calculate the instantaneous atmospheric density at the satellite's position. A GPS receiver on board a satellite provides the capability to acquire position and velocity data continuously and inexpensively. Thus, density can be determined throughout the satellite's orbit. Current methods to calculate atmospheric density use terrestrial observations and involve averaging through one or more orbits.

This project investigates the process in calculating atmospheric density from GPS data. A program is used to process the position and velocity data to compute density as a function of altitude. In the future, this program can be used to process GPS data on board satellites specifically designed for density measurements. With sufficient density data from numerous satellites, future scientists can use these data to develop a more accurate model of atmospheric density.

Background

Atmospheric density models are extremely valuable in astrodynamics applications. The major use of density models is for orbit propagation. With accurate models, it is possible to determine a satellite's future position with a high degree of certainty. There are a wide variety of models ranging from simplistic static ones to complex dynamic models. However, all of these models have substantial errors and deviate from actual conditions in varying degrees. The current density models are subject to errors of approximately 15%.[1] This accuracy is insufficient in many applications where more accurate orbit prediction is required. For example, the Air Force Space Command aims at knowing density within 5% of the actual value.[2]

The force due to drag is one of the major perturbing forces on satellites in low-Earth orbit where atmospheric density is the most variable factor. A low-Earth orbit (LEO) satellite is defined as a satellite that orbits the Earth at altitudes ranging from 300 km to 800 km above the Earth's surface. The drag force causes satellites to slowly spiral towards the Earth. Atmospheric drag makes precise orbit predictions difficult because atmospheric density is highly variable.

The most common density model is the exponential model. Density has been shown to decrease exponentially with height in accordance with the following equation[3]:

$$\rho = \rho_0 * e^{-\left(\frac{h_{act}-h_0}{H}\right)} \qquad (1)$$

where ρ is density, ρ_0 is a reference density, H is the scale height, h_{act} is the altitude of the satellite above the ellipsoidal Earth model, and h_0 is the reference altitude corresponding to the reference density. Scale height is a function of the atmosphere's composition at the

particular altitude. A change of one scale height results in a decrease of density by a factor of $\frac{1}{e}$. Although there is no standard reference for the exponential model, the altitudes and densities can be taken from existing models such as the U.S. Standard Atmosphere. For improved accuracies, the different reference altitudes, reference densities, and scale heights can be updated frequently. This exponential model is the most basic one, but is not adequate for high precision orbit predictions.

The deviations from the exponential model are caused by three main influences. These are latitude variations, diurnal variations, and the 11-year solar cycle. Latitude variations are caused by the Earth's oblateness. Since the Earth's equatorial diameter is approximately 20 km greater than the polar diameter, a satellite in a circular, inclined orbit will have a higher altitude at higher latitudes. Therefore, the satellite will pass through a region of higher density closer to the equator than at higher latitudes. Diurnal variations are caused by the Earth's rotation. The side of the Earth exposed to the sun is heated and the atmosphere expands. At a given altitude, the density is higher because the atmosphere is pushed up from the lower altitudes. On the nighttime side, the atmosphere cools and contracts and the density is less than the daytime side at a given altitude. Finally, the 11-year solar cycle affects the atmospheric density because the solar radiation varies with time. At the solar maximum, the sun releases more energy and the atmosphere expands as the Earth receives more radiation.

Atmospheric models have been created to account for these variations. Many atmospheric models in the past have been constructed using satellite drag analysis. However, these densities were derived by measuring the changes in the orbital elements

over at least one orbit. When measuring these changes, the calculated density is that at perigee. Yet even this value is an average in that the equations are averaged over one revolution. The resolution of the location where the density was calculated is approximately ± 20° centered at perigee due to the averaging.[4] Perigee is defined as a satellite's closest point of approach to the Earth, while apogee is the farthest point in a satellite's orbit, as seen in Figure 1.

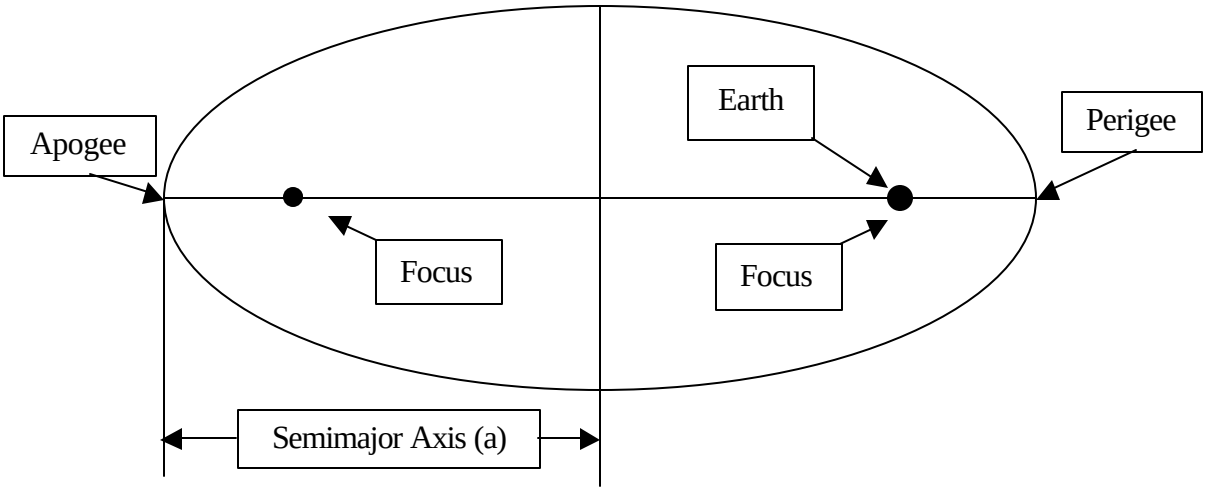

Figure 1: Diagram of an Elliptical Orbit

Another problem with earlier atmospheric models is the satellite tracking capabilities. According to Bruinsma[5], in the past,

> Orbit determination did not allow precise estimation of the satellite position at a given time essentially due to insufficient tracking capabilities as well as inaccurate gravity field models. Estimating the parameters over an orbit of several days was the only way to reduce random errors and geophysical noise, but at the cost of lesser resolution.

By using GPS receivers, orbit determination can be extremely accurate as well as continuous. Therefore, it is possible to determine the atmospheric density at a given point in a satellite's orbit since continuous satellite position and velocity measurements are available. Recent improvements in accuracies in GPS receivers have allowed for

many new applications for receivers. There are many types of GPS receivers available. One GPS receiver that is well suited for this application is the Ashtech G-12 HDMA GPS board. The position accuracy at orbital velocities is approximately 3.0 m Circular Error Probable (CEP) in the horizontal direction and 6.0 m in the vertical direction. The Ashtech receiver has a velocity accuracy of approximately 5 cm/s at orbital velocities.[6] This accuracy allows for precise orbit determination and GPS receivers can be used to determine atmospheric density. In addition, the G-12 HDMA board is qualified to orbital altitudes and velocities.

Theory

A satellite's orbit is defined by six parameters known as the classical orbital elements. These are the semimajor axis (a), eccentricity (e), inclination (i), longitude of ascending node (Ω), argument of periapsis, and true anomaly (n). The orbital elements can be calculated if the satellite's position and velocity are known. Figure 2 illustrates some of the classical orbital elements, while the terms are defined in Appendix A. In determining density, the semimajor axis, eccentricity, and true anomaly must be calculated.

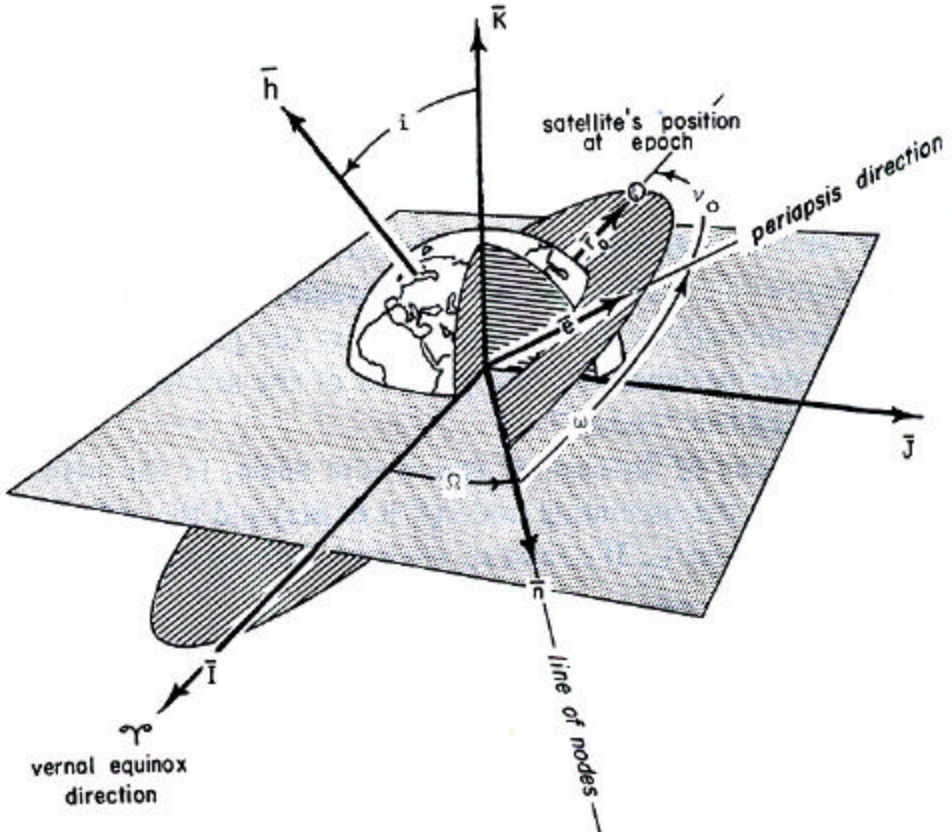

Figure 2: Classical Orbital Elements[7]

n_0 : True Anomaly
w : Argument of Periapsis
W : Longitude of Ascending Node
$\vec{e}$: Eccentricity Vector
i : Inclination

The semimajor axis defines the size of the orbit. Given position and velocity, the semimajor axis can easily be calculated. The specific mechanical energy of the orbit is defined in equation (2) by the sum of the specific potential and kinetic energies of the satellite:

$$\xi = \frac{v^2}{2} - \frac{\mu}{r} \tag{2}$$

where ξ is the specific energy, v is the magnitude of the velocity vector, r is the magnitude of the position vector, and μ is the Earth's gravitational parameter. The Earth's gravitational parameter is defined as the product of the Earth's mass and the gravitational constant in Newton's Universal Law of Gravitation. As shown by Vallado[8], once the energy is calculated, the semimajor axis (a) can be determined by using the following relationship:

$$a = -\frac{\mu}{2\xi} \tag{3}$$

The eccentricity measures the shape of the orbit. An orbit with an eccentricity of 0 defines a circular orbit and as the eccentricity increases towards 1, the orbit becomes more elliptical. The eccentricity vector ($\vec{e}$) is defined as:

$$\vec{e} = \frac{\left(v^2 - \frac{\mu}{r}\right)\vec{r} - (\vec{r} \bullet \vec{v})\vec{v}}{\mu} \tag{4}$$

The magnitude of the eccentricity vector represents the shape of the orbit, while the vector points in the direction of periapsis.

The final orbital element necessary in density calculations is the true anomaly. This is an angle measured from the eccentricity vector to the position vector as defined by the following equation:

$$\boldsymbol{n} = \cos^{-1}\left(\frac{\vec{e} \bullet \vec{r}}{|\vec{e}||\vec{r}|}\right) \tag{5}$$

where $\boldsymbol{n}$ is the true anomaly, $\vec{e}$ is the eccentricity vector and $\vec{r}$ is the position vector.

Atmospheric drag is a function of the atmospheric density, the satellite's coefficient of drag, cross sectional area, mass, and velocity relative to the atmosphere. The acceleration due to drag is given by the equation:

$$\vec{\mathbf{a}}_{drag} = -\frac{1}{2}\frac{C_D * A}{m}\boldsymbol{r} * \mathrm{v}_{rel}^2 * \frac{\vec{\mathbf{v}}_{rel}}{|\vec{\mathbf{v}}_{rel}|} \tag{6}$$

In equation (6), C_D represents the coefficient of drag, A is the cross-sectional area of the satellite, ρ is the atmospheric density, and v_{rel} is the satellite's velocity relative to the Earth's atmosphere. The satellite's ballistic coefficient is defined as $\frac{m}{C_D * A}$. As a satellite in LEO orbits the Earth, it experiences a force from atmospheric drag in the direction opposite the velocity vector.

By measuring the change in the semimajor axis, it is possible to calculate the density. In an equation developed from the Gaussian variation of parameters, Vallado[9] derives an equation for the time rate of change of the semimajor axis:

$$\frac{da}{dt} = -\boldsymbol{r}\frac{C_D * A}{m}\mathrm{v}_{rel}^2\left(\frac{\sqrt{1 + e^2 + 2 * e * \cos(\boldsymbol{n})}}{n * \sqrt{1 - e^2}}\right) \tag{7}$$

In this equation, the time rate of change of the semimajor axis, $\frac{da}{dt}$, is a function of the ballistic coefficient, density, relative velocity, eccentricity, true anomaly, and mean motion. A derivation of equation (7) can be found in Appendix D. Mean motion, a function of the semimajor axis and the Earth's gravitational parameter, is defined as:

$$n \equiv \sqrt{\frac{m}{a^3}} \tag{8}$$

Solving equation (7) for density,

$$\rho = -\frac{da}{dt} * \frac{m}{C_D * A} * \frac{1}{v_{rel}^2} * \left(\frac{n * \sqrt{1-e^2}}{\sqrt{1+e^2+2*e*\cos(\theta)}} \right) \tag{9}$$

The terms in equation (9) can be calculated from position and velocity information with the exception of the ballistic coefficient and the time rate of change of the semimajor axis. The ballistic coefficient can be variable depending on the mass of the satellite and its orientation. If the satellite has a propulsion system, the mass will decrease as fuel is expended, thus changing the ballistic coefficient with time. The cross-sectional area can change if the spacecraft's orientation is changing with respect to the atmosphere and the direction of motion. To eliminate these variables, the satellite used to determine the density must have a constant mass as well as a constant cross sectional area. Therefore, the satellite would be designed with no propulsion system. To eliminate orientation problems, the satellite would be designed to be spherically symmetric. Finally, the coefficient of drag can be approximated as 2.2 for spherical satellites.[10] The time rate of change of the semimajor axis is the most important variable in equation (9). To obtain

the term $\frac{da}{dt}$, the numerical derivative of the semimajor axis with respect to time must be calculated.

Several assumptions were made when calculating the atmospheric density. In equation (9), the time rate of change of the semimajor axis must be isolated due to drag only. However, the other major perturbing force on a satellite in LEO is due to the Earth's geopotential. The Earth is shaped as an oblate spheroid thus its gravitational field is not a perfect sphere. The Earth's asymmetric gravitational field causes perturbations in a satellite's orbit and it affects the semimajor axis with periodic variations. To determine the change in the semimajor axis due to drag, I assumed the effects on the semimajor axis due to the Earth's geopotential and drag were independent. Thus, to determine the changes in the semimajor axis due to drag, the effects of the geopotential could be algebraically subtracted from the data. This assumption was found to be incorrect as seen in the Results and Discussion section; however, by limiting the length of time in which the two were subtracted, the differences were reasonable. Thus, the assumption was adequate for this application.

Another assumption is that the only major forces on the satellite are drag and the geopotential. Outside forces such as third-body effects and solar radiation are assumed to be much smaller than these forces and do not affect the satellite. This is reasonable in that in low-Earth orbit, in this case, at altitudes below 500 km, these forces are small. This can be seen in Figure 3 for an orbit with a semimajor axis of 6878 km.

The third-body effects of the sun and moon as well as the effect of solar radiation

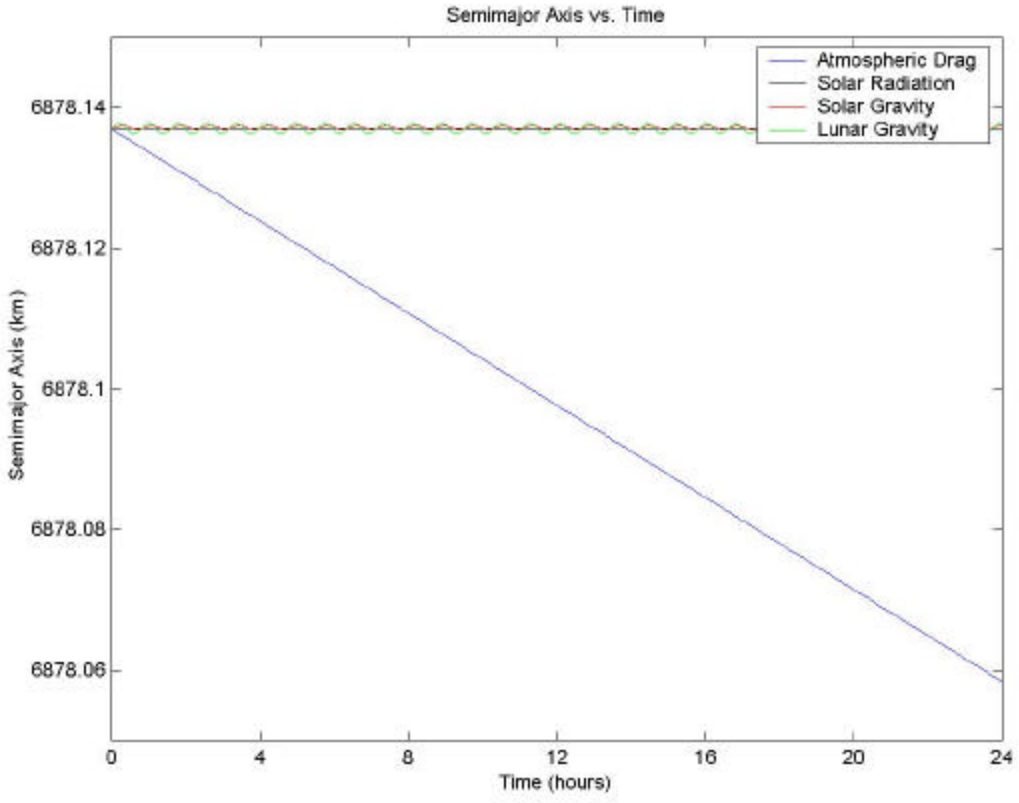

Figure 3: Periodic Effects on the Semimajor Axis of Third-Body Perturbations and Solar Radiation Compared with Atmospheric Drag

are periodic and much smaller than the effect of atmospheric drag. Therefore, the perturbations which affect the semimajor axis the most are atmospheric drag and the Earth's asymmetric gravity field. The effects of the Earth's gravity field will be shown in the Results and Discussion section of this report.

The final assumption was that the atmosphere was rotating with the Earth. This assumption is reasonable in that the U.S. Standard Atmosphere models the atmosphere to rotate with the Earth. In addition, the atmosphere is not stationary and rotates at velocities up to the Earth's rotational velocity. Equations developed by King-Hele[11] were used to model the rotating atmosphere in my algorithm. These equations can be found in Appendix E.

Methodology

I developed several steps in my algorithm to calculate atmospheric density. These steps were:

1. Rotate the GPS data into the Geocentric Equatorial Frame
2. Calculate orbital elements from GPS data
3. Calculate the satellite's relative velocity.
4. Isolate the effects of drag on the semimajor axis
5. Calculate the time rate of change of the semimajor axis
6. Calculate the atmospheric density

First, GPS data must be processed to determine the classical orbital elements. I used Satellite Tool Kit®[12] to simulate the GPS data in the form of position and velocity in the Earth-Centered, Earth-Fixed coordinate frame. In addition, time and altitude are also included in the simulated GPS data. These data included effects of the Earth's geopotential and atmospheric drag. The disturbing potential for the Earth's nonspherical shape is given by the following equation:

$$U = \frac{m}{r}\sum_{l=0}^{\infty}\sum_{m=0}^{l}\left(\frac{R_{\oplus}}{r}\right)^{l} P_{lm}[\sin(\phi_{SAT})]\{C_{lm} * \cos(m\lambda_{SAT}) + S_{lm} * \sin(m\lambda_{SAT})\} \qquad (10)$$

where m is the Earth's gravitational parameter, r is the magnitude of the satellite's position vector, $R_{\oplus}$ is the Earth's radius, $P_{lm}[\sin(\phi_{SAT})]$ is the associated Legendre function, ϕ_{SAT} is the satellite's latitude, λ_{SAT} is the satellite's longitude, and C_{lm} and S_{lm} are coefficients that model the Earth's spherical harmonics[13]. In equation (10), l and m describe the degree and order of the geopotential model. Satellite Tool Kit® uses the Joint Gravity Model (JGM) 2 as its geopotential model. In my analysis, I used a 70x70 (l x m) geopotential model and the 1976 Standard Atmosphere to generate the GPS data.

Initially a time step of 60 seconds was used over one orbit, yielding approximately 90 data points.

With the simulated GPS data, position and velocity were rotated from the Earth-Centered, Earth-Fixed frame to the inertial Geocentric Equatorial frame. In addition, the velocity of the satellite relative to the atmosphere was calculated. Following this, the classical orbital elements were calculated at each time step. These data show how the orbital elements, mainly the semimajor axis, vary with time. However, these data include effects of the geopotential with drag. For density analysis, the changes in semimajor axis with respect to time due to drag are needed.

To obtain the changes in the semimajor axis due to drag only, I ran two more STK® simulations. The first was the same orbit, however, only due to the geopotential effects, while the second was the two-body case. The two-body case is defined by assuming the Earth and the satellite are point masses. The other assumption in the two body case is that the satellite is not subjected to any forces other than gravity of the Earth. With each of these two runs, STK® output the semimajor axis. I then subtracted out the semimajor axis effects due to the geopotential from the semimajor axis due to the geopotential and drag. Finally, to obtain the semimajor axis due to drag only, I algebraically added the semimajor axis of the two-body case.

The next step in the process is to determine the time rate of change of the semimajor axis. To do so, I used the MATLAB®[14] function "polyfit" to model the variation of the semimajor axis with respect to time as a polynomial. With this polynomial, I took the numerical derivative to obtain the time rate of change of the semimajor axis. With this information, all of the values in equation (9) are known.

Density as a function of time and more importantly, density as a function of altitude can be determined.

Results and Discussion

In conducting my research, I was able to calculate atmospheric density, obtaining percent errors consistently below 1% when compared to the 1976 Standard Atmosphere model. However, in the process there were several phenomena I had not anticipated. These were the geopotential effects, latitude effects, and the atmospheric rotation. Once my algorithm was generating density values corresponding to the input model, I added random noise into the GPS data. I also included complex density models such as the Harris-Priester, Jacchia-Roberts, Jacchia 1960, and Jacchia 1971 models in the STK® simulations. With these models, diurnal variations, geomagnetic variations, and the effects of the 11-year solar cycle, were examined with respect to changes in the atmospheric density.

I produced plots of density vs. altitude for several different orbits. These included circular equatorial, circular inclined, eccentric equatorial, and eccentric inclined orbits. In addition, the semimajor axis was varied to account for altitudes between 250 km and 400 km. Figure 4 shows a plot of density vs. altitude for the circular equatorial case, with an initial semimajor axis of 6678 km. In the plots of density vs. altitude, the "Drag Analysis" case represents the output of my algorithm. Figure 5 plots the percent error vs. time for the same case. The errors with the circular equatorial case are under 1% and remain below the 1% bound for one orbit. Corresponding plots for inclined orbits are presented in Appendix B. The percent error in the calculated density for an inclined orbit began within the 1% error bound, but the inclined orbits were subject to an increasing error in the calculated density as time progressed. The increasing errors were due to the assumption that effects of the geopotential on the semimajor axis were independent of the

effects of drag. The variations in the semimajor axis due to the geopotential are a function of inclination because of the shape of the Earth. The following plots (Figures 4 and 5), along with others found in Appendix B, represent the final output of my algorithm.

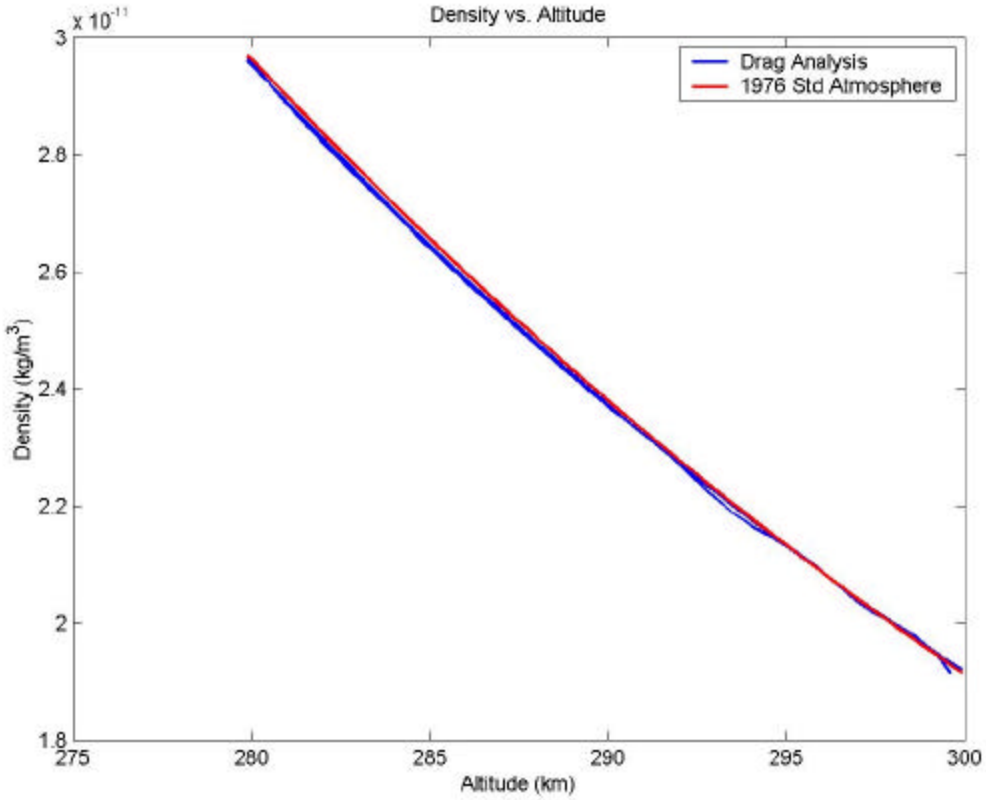

Figure 4: Calculated Density and Reference Density vs. Altitude: Circular Equatorial Orbit

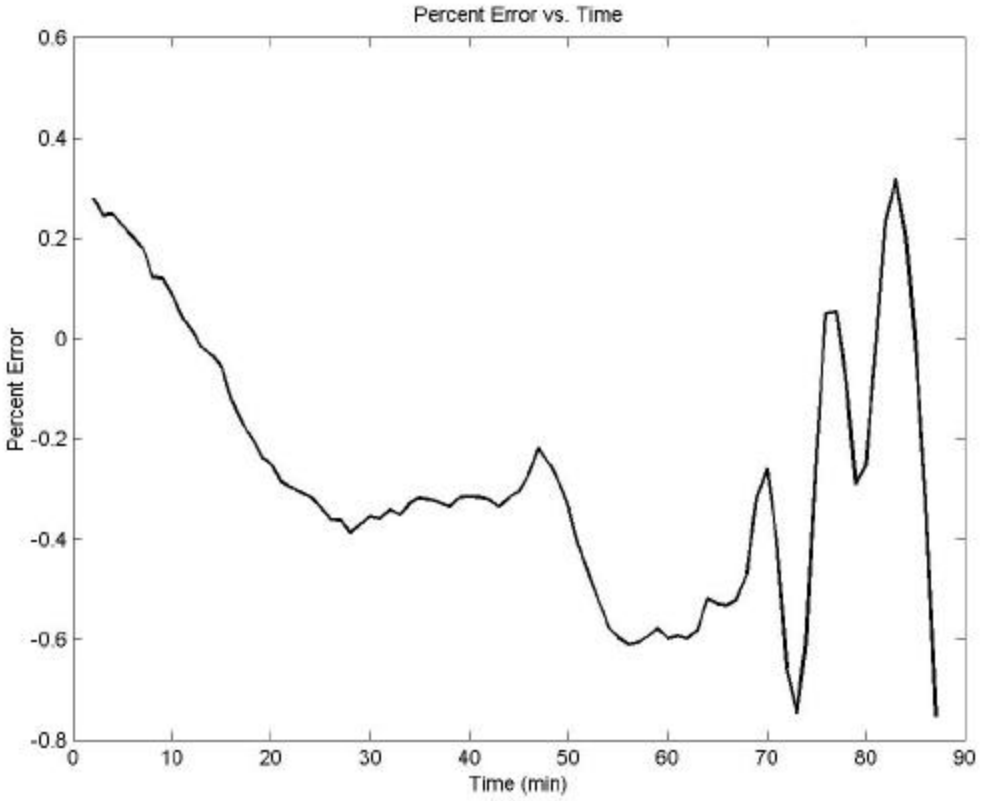

Figure 5: Percent Error in Density vs. Altitude: Circular Equatorial Orbit

Geopotential Effects

The first major finding was that changes in the semimajor axis due to drag and the geopotential were not independent and that the initial assumption was incorrect. Analysis using STK® demonstrated that there was a coupling between the two forces as shown by Figure 6. This plot shows the semimajor axis of a satellite in a circular orbit with an inclination of 30°. The effects of the geopotential are periodic and cause the semimajor axis to vary in magnitude. The straight line in Figure 6 plots the semimajor axis in the two-body case, where the Earth is modeled as a perfect sphere, and thus, has a uniform gravity field. The sinusoidal line shows the periodic effects of the geopotential on the semimajor axis.

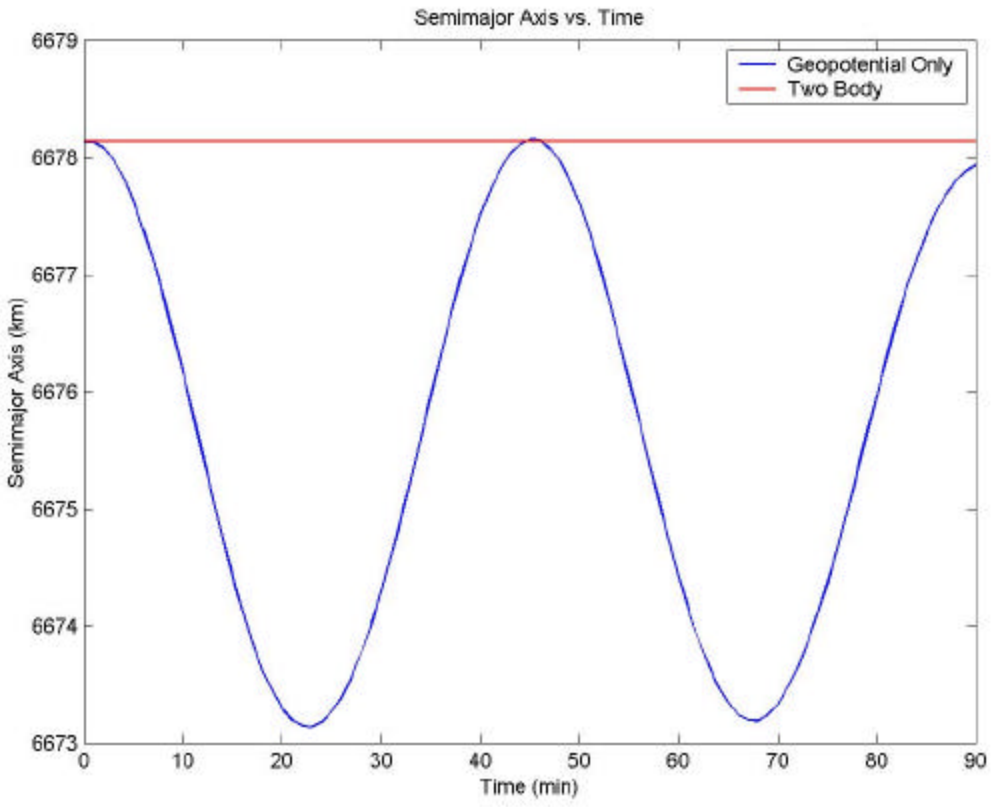

Figure 6: Periodic Variations in the Semimajor Axis Due to the Earth's Geopotential

The coupling of the changes in semimajor axis due to the geopotential and drag can be seen in Figures 7 and 8. Figure 7 plots the changes in the semimajor axis due to the geopotential as well as due to the geopotential combined with drag. The plot of the changing semimajor axis due to the geopotential and drag combined shows that there is a decrease as time progresses.

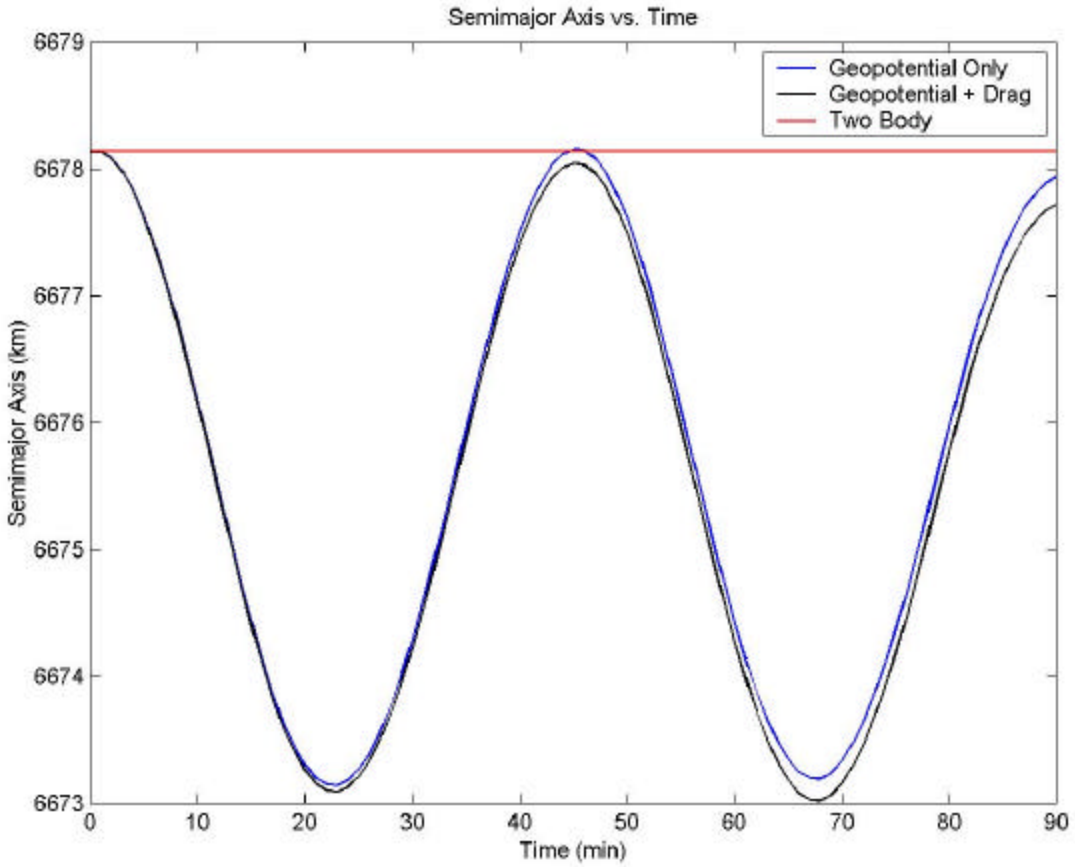

Figure 7: Variation in the Semimajor Axis due to the Earth's Geopotential and Geopotential and Drag

The coupling can be seen in Figure 8, where the semimajor axis that was calculated decreases, but has periodic variations as it decreases. The periodic effects are due to the coupling with the geopotential. As the satellite's semimajor axis decreases, the density

increases, and therefore the rate at which the semimajor axis decays due to drag increases as well. Therefore, the rate at which semimajor axis changes due to drag is not constant. As time progresses, the differences between the pure drag case and the approximated drag case increase. The pure drag case is where the only perturbation input into STK® was atmospheric drag. In the approximated drag case, the semimajor axis was calculated by algebraically subtracting the geopotential only case from the case of the geopotential combined with drag.

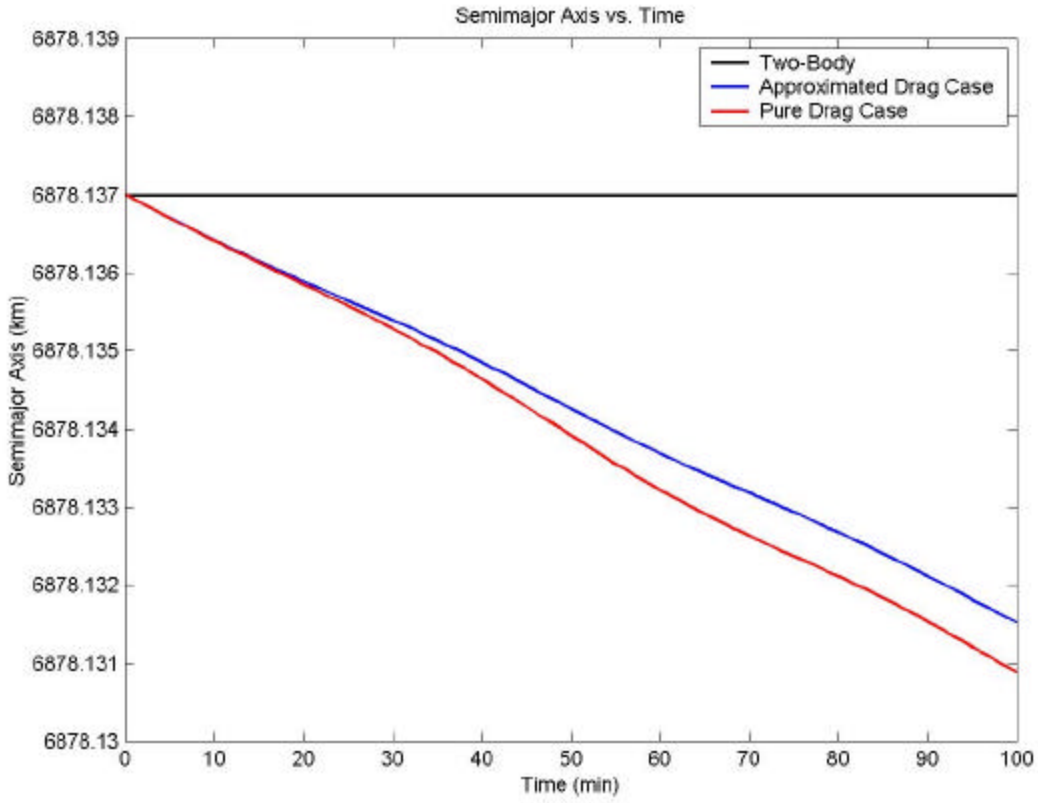

Figure 8: Variation in the Semimajor Axis Due to Drag: Calculated and Pure Drag

To correct for the error growth, I determined that by limiting the length of time for the data collection to half of a period, the differences between the two cases are within reasonable bounds of 1%. Once the satellite has made one half of a revolution, the

new semimajor axis is input into the STK® simulation so that the deviations do not increase to an unreasonable magnitude. The coupling between the effects of the geopotential and drag are responsible for the increasing errors in my density calculations. In the circular equatorial case, the low percent error of 1% can be attributed to the negligible geopotential effects. Since the inclination is zero, the magnitude of the variations in semimajor axis are insignificant and thus it is not a major source of error. For inclined orbits, the errors increase with time as shown in Figure 9. This plot is of a circular orbit with an inclination of 30°. Goals for the errors in the density calculation were set to be less than or equal to 1%. Table 1 indicates the values of the errors with time. Errors remain at a reasonable level of 1% through approximately half a revolution. Past this point, the errors continue to grow. Past one revolution, the errors become inadequate for accurate density analysis. Therefore, the orbital elements must be updated at a minimum of half a revolution to ensure errors of 1% or less.

Table 1: Long-Term Errors in Density Calculations

Time	Error (%)
1/4 Orbit	< 0.5
1/2 Orbit	1
3/4 Orbit	3
1 Orbit	5
2 Orbits	19

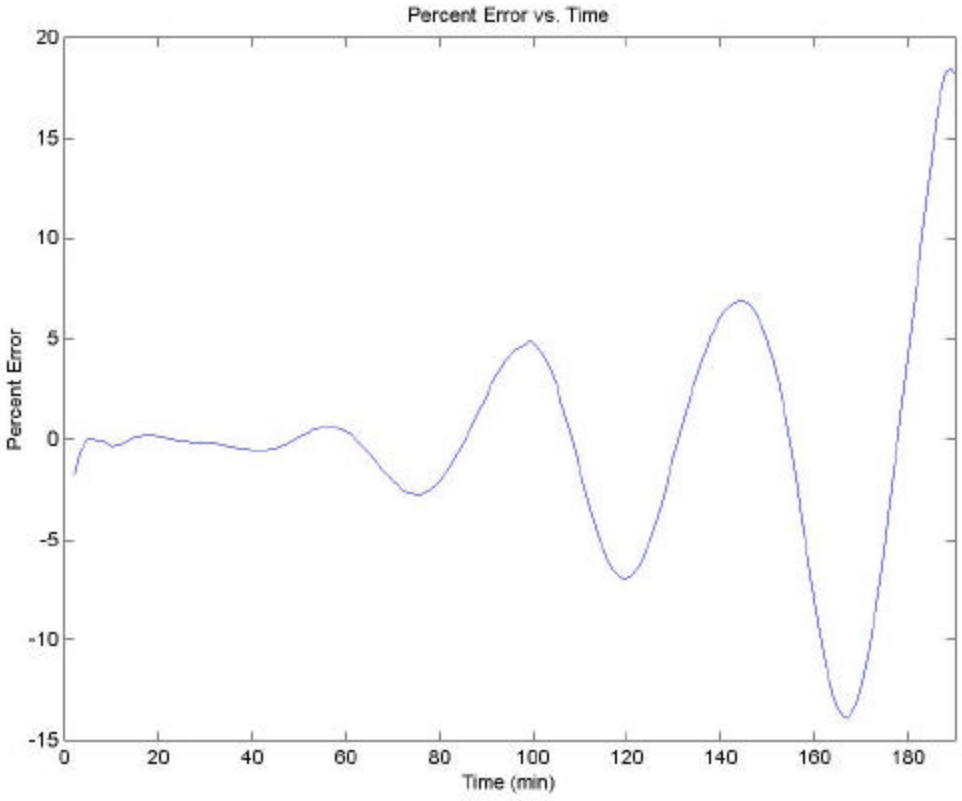

Figure 9: Long Term Percent Error: Circular Inclined Orbit (Inclination 30°)

Latitude Effects

Latitude effects on density calculations played a large part in the accurate density calculations. Initially, to determine the satellite's altitude I subtracted the magnitude of the satellite's position vector from the Earth's radius. Thus, the calculated altitude represented that for a spherical Earth rather than the actual oblate Earth. As seen in a circular inclined case in Figure 10, the density corresponds near perigee and apogee (300 and 283 km), where the satellite is at the equator. During the course of an orbit, the satellite begins at an apogee of 300 km, and decreases in altitude to approximately 283 km at perigee. The satellite then returns to its initial altitude of 300 km. In this case, the satellite's inclination is 30°. However, as the satellite increases in latitude, the actual altitude is higher than the calculated altitude. Therefore, the calculated density is lower between perigee and apogee than the actual values.

By using STK® generated altitudes that took the Earth's oblateness into account, the calculated density corresponded with the U.S. Standard Atmosphere model. The addition of the altitude information is reasonable because GPS has the capability of outputting the altitude of the receiver, where the altitude is referenced to an accurate ellipsoidal Earth model.

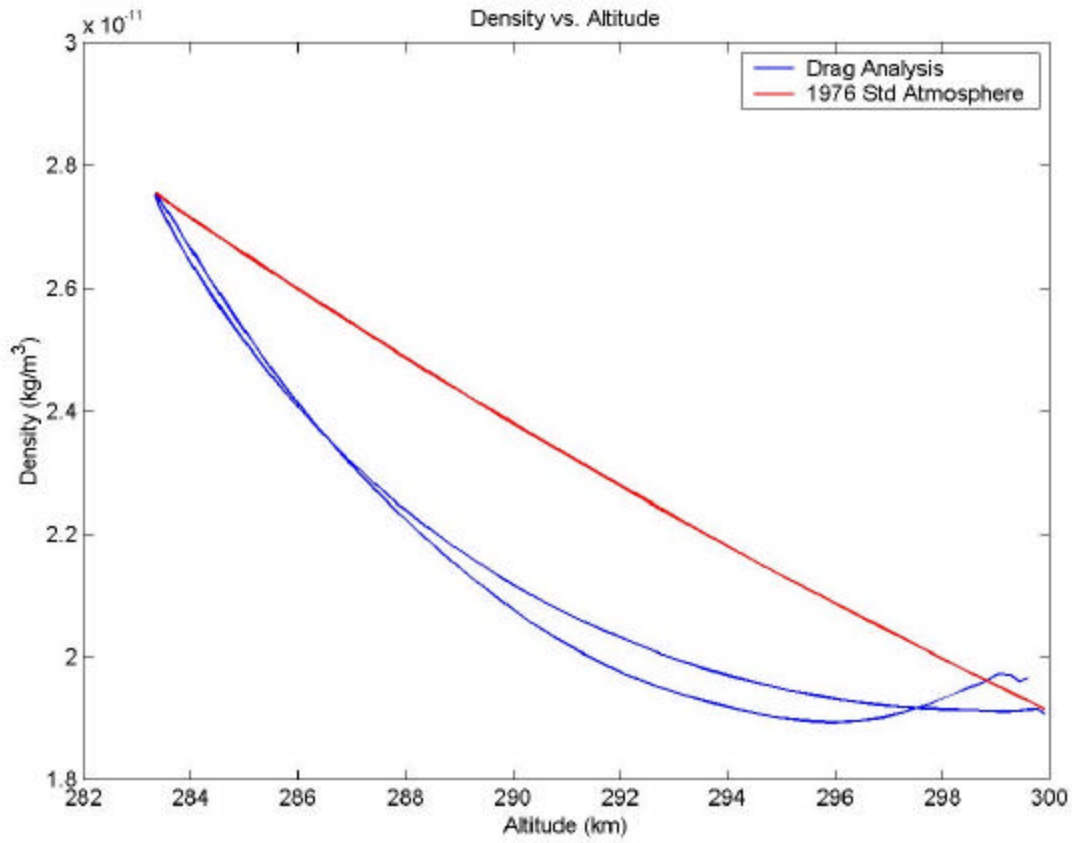

Figure 10: Latitude Effects on the Calculated Density: Circular Inclined Orbit

Atmospheric Rotation

The rotating atmosphere also affects density calculations. Although the value of the atmosphere's velocity is small when compared to the satellite's velocity, the effect on the calculated density can cause an error as large as 12%. The effects of the atmospheric rotation can be seen in the following three plots, Figures 11, 12, and 13. These three density calculations assume a non-rotating atmosphere. Figure 11 shows density calculations for a direct orbit, where the satellite has an inclination of 0° . The plot shows a consistent error of approximately 12% below the reference densities. In the case of a direct orbit, the satellite's relative velocity is lower than its inertial velocity. Thus, the calculated densities are lower than the reference densities.

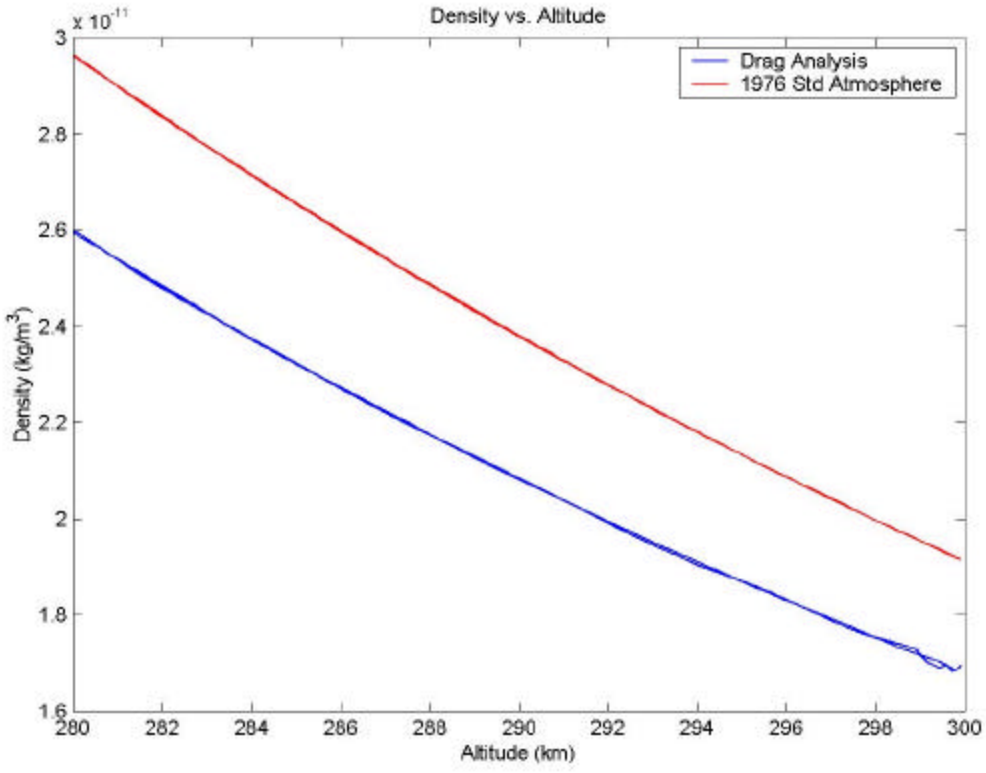

Figure 11: Calculated Density and Reference Density vs. Altitude: Circular Equatorial Orbit

The next plot, Figure 12, shows density calculations from a polar orbit, which has an inclination of 90°. In this run, the calculated density corresponds with the U.S. Standard Atmosphere densities, however the errors increase as time progresses. It is assumed in this case that the satellite's velocity vector is perpendicular to the atmosphere's velocity, and does not have an effect of the density calculation.

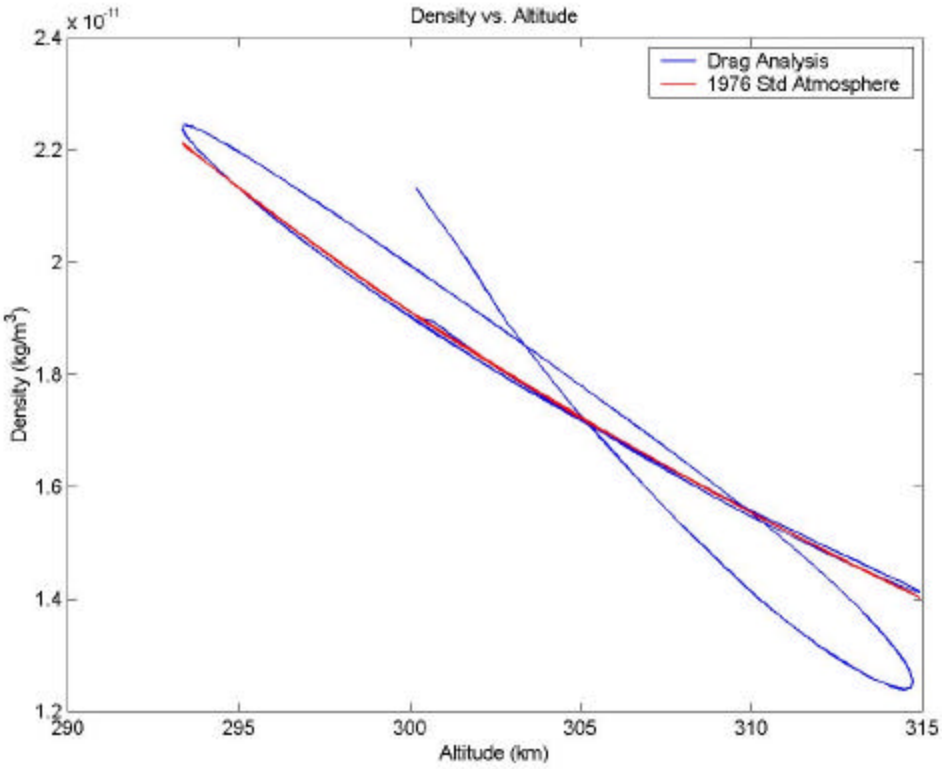

Figure 12: Calculated Density and Reference Density vs. Altitude: Circular Polar Orbit

Finally, Figure 13 shows a retrograde orbit with an inclination of 180°. In this case, the satellite is going "against" the wind and the relative velocity is lower than its inertial velocity. This plot has an error of 12% when compared to the reference densities;

however unlike the direct orbit, the calculated densities are higher than the reference densities.

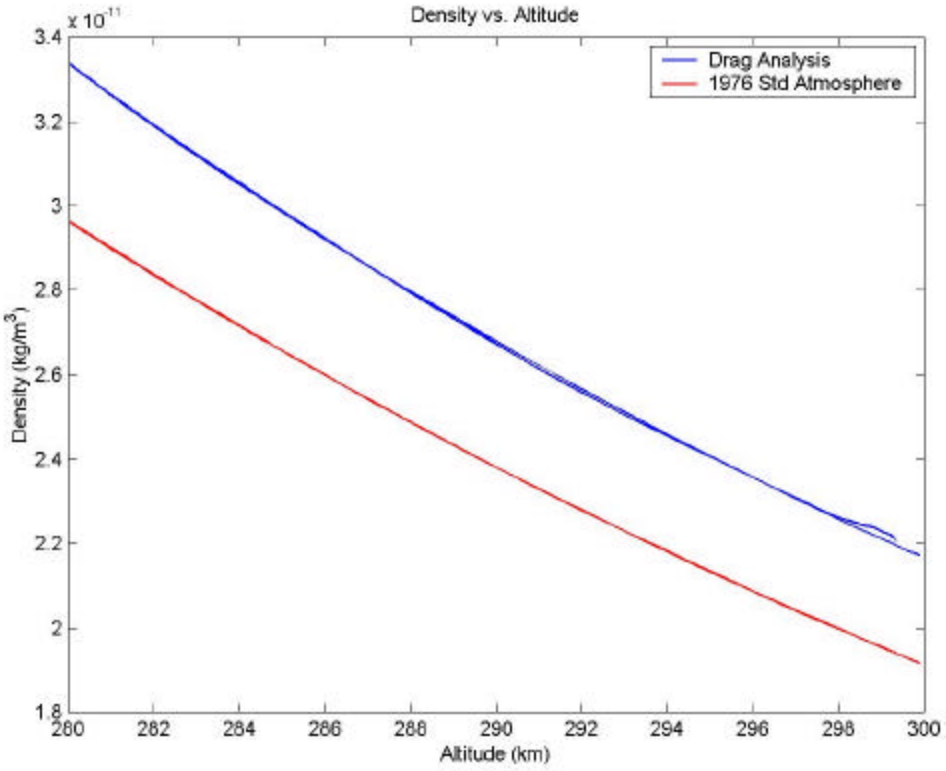

Figure 13: Calculated Density and Reference Density vs. Altitude: Circular Equatorial (Retrograde)

These three plots demonstrate that there is a significant effect on the density calculations and that is a function of the satellite's inclination. Since the direct orbit and the retrograde orbit produce errors of the same magnitude, but different signs, the atmosphere's velocity influences the calculations considerably. Once the atmosphere's velocity was accounted for, the errors were significantly reduced.

Complex Atmospheric Models

There are many atmospheric models that include complex features of the atmosphere such as the effects of diurnal variations, varying solar flux, and geomagnetic activity. The algorithm developed illustrates these variations quantitatively. Although the calculated density values are not validated with the corresponding models, the patterns are consistent with expected trends. Atmospheric density reaches its maximum at approximately 1400 local solar time[15]. This trend is illustrated in Figure 14. This figure plots four runs where a different atmospheric model was used in the orbit propagation. The orbit used in Figure 14 is a circular equatorial orbit with a semimajor axis of 6678 km. The models used were the Harris-Priester, Jacchia-Roberts, Jacchia 1960, and Jacchia 1971 models. In these models, variations in the density values are a result of the different density data collected and used to create the models. All of them show the basic trends in density with time, however some include more complex inputs such as the solar flux level and the geomagnetic activity. The geomagnetic activity refers to the strength of the Earth's magnetic field.

The diurnal variations are clearly defined by all four models. The peaks in Figure 14 were found to correspond to approximately 1400 local solar time. The actual values of density differ between the models; however, they are on the correct order of magnitude for the satellite's altitude.

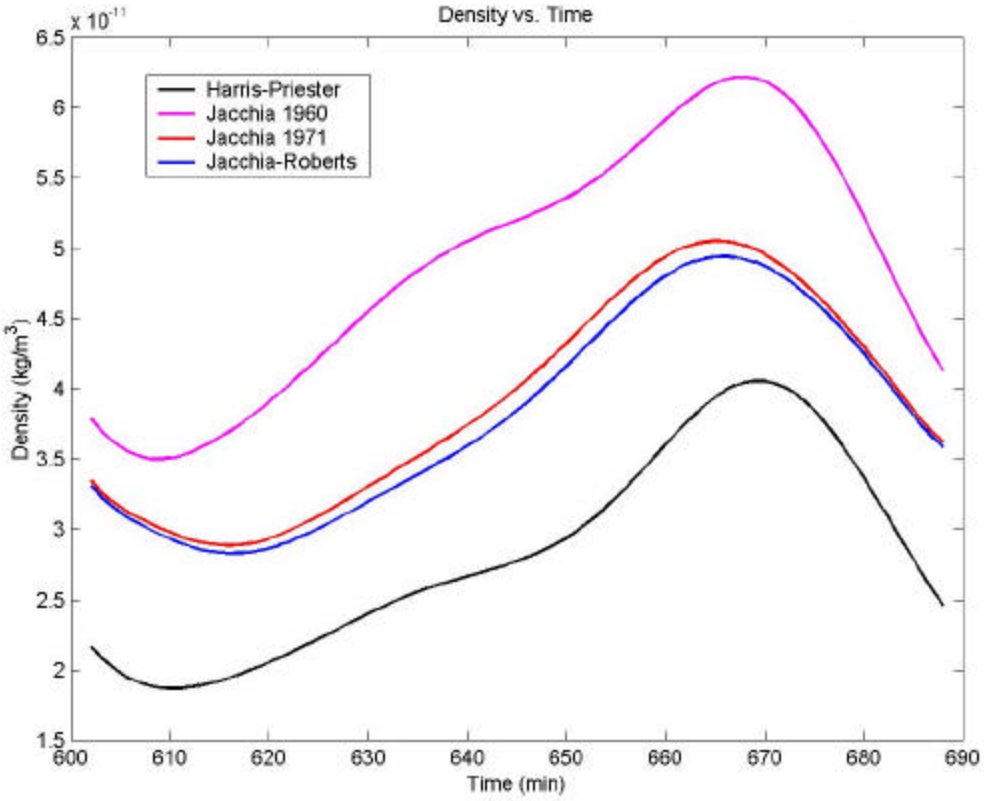

Figure 14: Calculated Densities as a Function of Time using Four Different Atmospheric Models

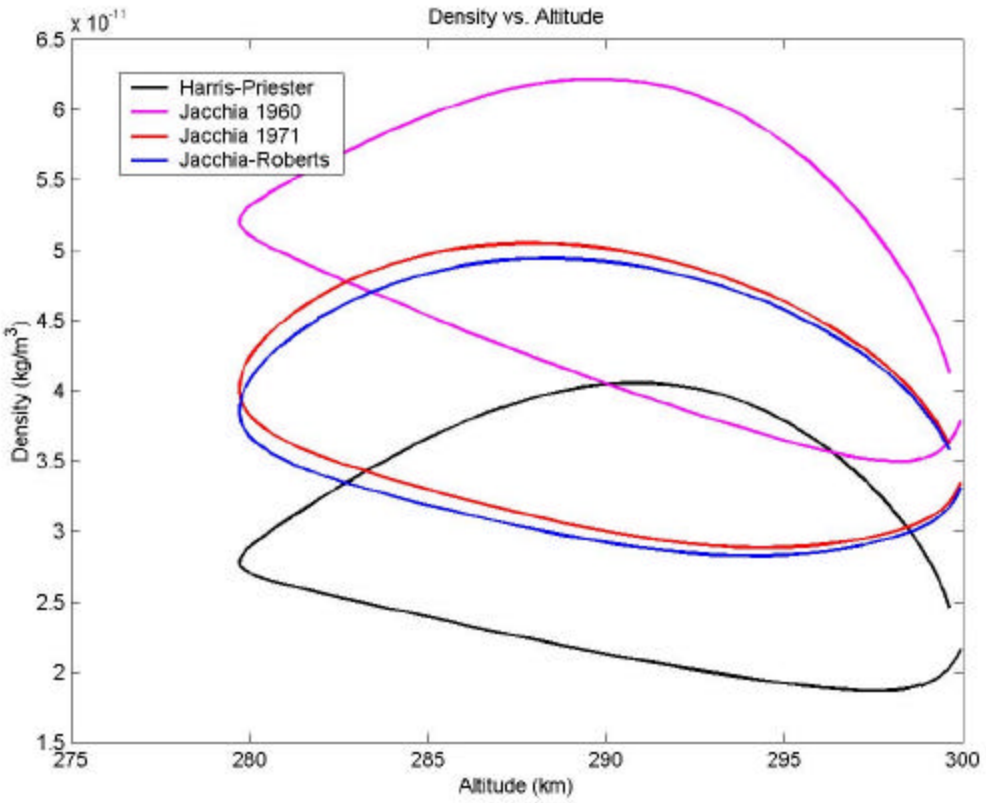

Figure 15: Calculated Densities as a Function of Altitude using Four Different Atmospheric Models

Figure 15 plots density vs. altitude for the same case in Figure 14. Figure 15 demonstrates the similarity among the four models where the increases are similar. The Jacchia 1971 model and the Jacchia-Roberts model closely match each other in this run. The similarity is because the Jacchia-Roberts model is a modification of the Jacchia 1971 model.

Many atmospheric models account for variations in the solar flux. Figure 16 plots three STK® runs using the Harris-Priester model. The runs differed by the solar flux input into the propagator.

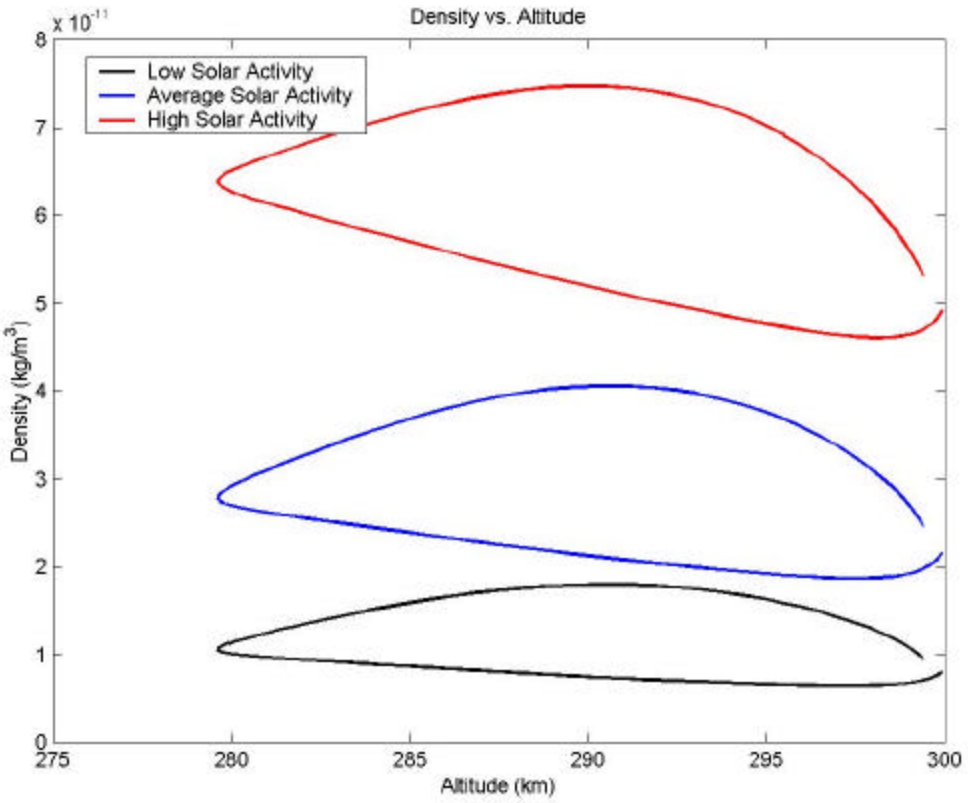

Figure 16: Solar Flux Effects on Atmospheric Density

The three values for the low, average, and high solar flux inputs were 65 x 10^{-22}, 150 x 10^{-22}, and 250 x 10^{-22} W/m^2 Hz respectively. Figure 16 shows that as the solar flux increases, the density at a given altitude increases as well.

The last major variation in density taken into account by some models is the effects of the geomagnetic activity. A higher geomagnetic index causes the density at a given altitude to increase, while a lower geomagnetic activity relates to a lower density at a given altitude. Figure 17 illustrates three runs with different values for the geomagnetic index. The geomagnetic index is a value used to describe the activity, where a higher number indicates the geomagnetic activity.

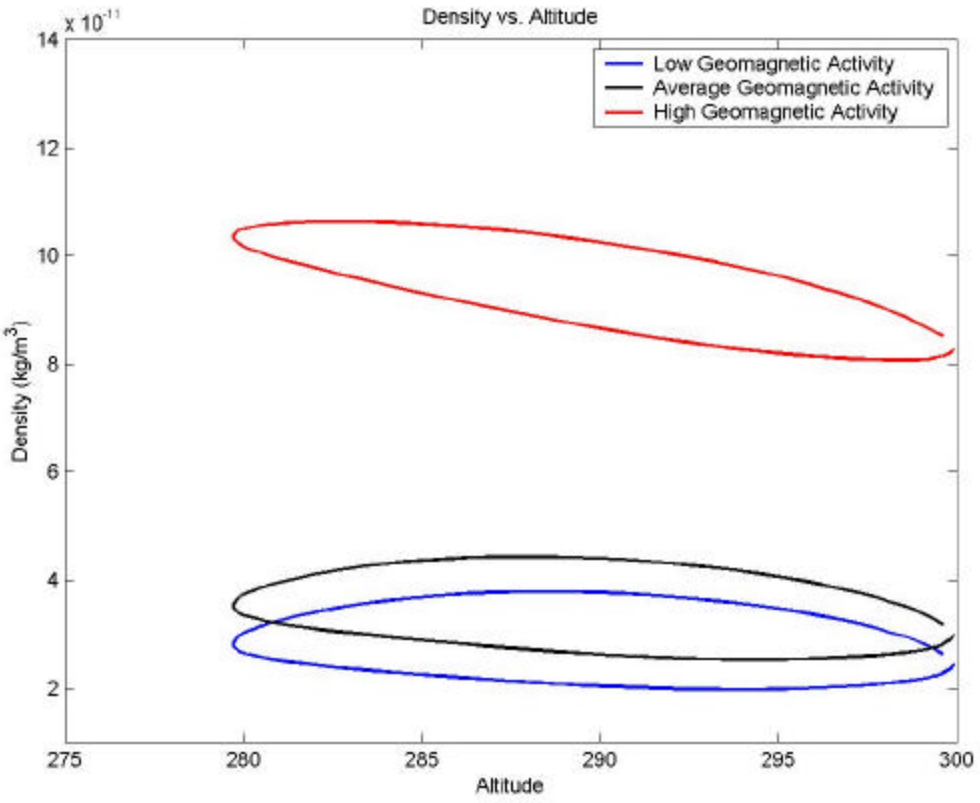

Figure 17: Geomagnetic Activity Effects on Atmospheric Density

The density calculation algorithm that was developed demonstrates the complex variations in density among different models. Since these models are complex and determining density values involves interpolations among different tables, it is difficult to accurately determine the error in the calculated density and reference density. However, based on the errors in the density as compared with the 1976 Standard Atmosphere, one can expect the errors to increase with time.

Errors

In the density analysis, there are several sources of error. These errors are a result of uncertainties in equation (9). In the STK® simulation, values of position, and velocity are calculated as a result of the propagation. In addition, the coefficient of drag (C_D) remains a constant value. However, realistic conditions add errors into these values. For example, the position and velocity data obtained from the GPS receiver will deviate from the true positions resulting from errors in the receiver's accuracy. For the Ashtech G-12 HDMA GPS receiver board, errors of 3.0 m CEP and 6.0 m in altitude can be expected.

The error in the time rate of change of the semimajor axis is low compared to other possible sources of error. In order to calculate the time rate of change of the semimajor axis, I used MATLAB® to fit a polynomial to the semimajor axis vs. time plot. A second order polynomial was used to fit five data point sections on the curve of semimajor axis vs. time. By taking the derivative of the polynomial, the time rate of change of the semimajor axis was determined.

When random errors are introduced to the STK® simulated data, errors in the calculated density are greater than 1% and are deemed unacceptable. The errors are present because the orbital elements calculated from the position and velocity data vary greatly. As a result, the derived semimajor axis does not vary consistently with a satellite decaying in the atmosphere. Thus, the time rate of change of the semimajor axis due to atmospheric drag is not accurately represented. When processing raw data from a GPS receiver, a smoothing algorithm is necessary to eliminate the random noise in the GPS receiver. Barring effects of the random noise on the semimajor axis, the maximum

predicted error of 6 meters in altitude will result in an error in density by approximately 0.02%.

Another possible source of error is the coefficient of drag. In low-Earth orbit, the coefficient of drag for a sphere can be approximated to be 2.2, however, errors in this value can be as much as 10%[16,17]. The variations in the coefficient of drag are largely a function of the atmospheric composition. Thus, a 10% error in the correct value of the coefficient of drag results in a 10% error in the calculated density.

Finally, the last major source of error lies in the motion of the atmosphere. The atmosphere is assumed to rotate with the Earth, with rotational velocity bounds of zero and the Earth's angular velocity. At lower altitudes, the atmospheric velocity is higher due to friction[18] and as the altitude increases, the velocity decreases towards zero. In the 1976 U.S. Standard Atmosphere model, the entire atmosphere is modeled to rotate with the Earth. In initial runs of my density calculations, I assumed that the velocity of the atmosphere was zero. With this assumption, the maximum errors were approximately 12%. Therefore, errors in the density calculations due to the variations in the atmospheric velocity can be assumed to be within 12%.

Spacecraft Design

The driving requirements in designing a spacecraft to carry out the mission of collecting data to determine atmospheric density are the payload as well as the shape and mass. The primary payload is an accurate GPS receiver to determine the position and velocity of the satellite. However, another major requirement for the satellite is to maintain a constant ballistic coefficient. To accomplish this, the satellite's mass must not change and its cross sectional area and coefficient of drag must remain constant as well. Therefore, the best configuration for the spacecraft would be a spherical shape with no propulsion system. This would ensure that the ballistic coefficient remains constant in any orientation.

A proposed GPS receiver for the spacecraft is the Ashtech G-12 High Dynamics and Missile Applications (HDMA) receiver board. The Ashtech receiver is qualified to orbital velocities as well as altitudes. The receiver is also small and lightweight making it ideal for a small satellite design. In addition, the power requirement of 1.8 W is suitable for satellite operations. Estimated accuracies at orbital velocities for the receiver are 3.0 m CEP for position and 0.05 m/s for velocity.

The mission of the spacecraft lends itself to a "store and forward" communications architecture. As the satellite orbits the Earth, it will take position and velocity readings from the GPS and store them into a storage device on the spacecraft. Using STK®, readings every 60 seconds is sufficient to determine the atmospheric density in the orbit. However, readings every 30 seconds or less would allow increased accuracy and filtering of random noise. Once the satellite passes over the U.S. Naval Academy and downloads its stored data, the stored position and velocity can be erased on

the spacecraft. Once downloaded to the ground station, the data will be processed to determine the densities in the satellite's orbit.

Currently, the U.S Naval Academy Small Satellite program is in the process of designing the Prototype Communications Satellite or PC-Sat. This satellite will be testing a GPS receiver developed by the German Space Operations Center. With this payload, position and velocity data can be retrieved and saved. Although the ballistic coefficient will not be constant due to its shape, the opportunity exists for testing data processing techniques. Upon launch of the satellite designed to determine atmospheric density, data processing methods can be in place to calculate atmospheric density immediately.

Conclusions

My work has demonstrated that it is possible determine the atmospheric density in a satellite's orbit using a GPS receiver. Several assumptions are necessary to yield accurate results. Most of these assumptions are reasonable; however, the assumption that the atmosphere rotates with the Earth has the potential for creating the highest error. The atmosphere has a velocity that can range from zero to the Earth's rotational speed. With an accurate model of the atmospheric winds, it would be possible to determine density more accurately. Based on the bounds placed on the atmospheric winds, the greatest possible error in my algorithm is 12%. This error is too large to allow reasonable calculations of density and therefore, future modifications must be made.

For my algorithm to be suitable for the USNA small satellite program, my algorithm should include a filter to eliminate the noise from the GPS data. Even small inaccuracies in the GPS data cause large errors in the density calculations. Another improvement to my algorithm would be to eliminate the need for Satellite Tool Kit®. By programming a propagator into the algorithm, it will simplify the density analysis because frequent updates of the orbital elements could be done automatically. In addition, the orbital element updates could be done more frequently, driving the errors down significantly. This project has laid the groundwork for the next generation of the USNA small satellites. With the suggested modifications, future Midshipmen can use the algorithm to create a database for scientists to use in creating a new, more accurate atmospheric density models.

Endnotes

[1] F.A. Marcos et al., "Precision Low Earth Orbit Determination Using Atmospheric Density Calibration." The Journal of the Astronautical Sciences, Vol. 46, No. 4, October-December 1998, p 396.

[2] Ibid, 396.

[3] David A. Vallado, Fundamentals of Astrodynamics and Applications, New York: The McGraw Hill Companies, 1997, 509.

[4] M. Roemer, "Recent improvements in our knowledge of neutral atmosphere structures from satellite drag measurements." Radio Science, February 1974, vol. 9. no. 2, 224.

[5] S.L. Bruinsma, P. Exertier, R. Biancale. "An Assessment of New Satellite Total Density Data for Improving Upper Atmosphere Models." Planetary and Space Science, 47 (1999) 1467.

[6] Magellan Corporation, Ashtech G-12 HDMA GPS Board Information.

[7] Roger R. Bate, Donald D. Mueller, and Jerry E. White, Fundamentals of Astrodynamics, New York: Dover, 1971, 59.

[8] Vallado, 109.

[9] Vallado, 559-561, 604-605.

[10] Desmond King-Hele, Satellite Orbits in an Atmosphere: Theory and Applications, London, England: Blackie and Son, Ltd, 1987, 25.

[11] Ibid, 30.

[12] Satellite Tool Kit® Ver 4.1.1b, Analytical Graphics Inc. 2000.

[13] Vallado, 485-494..

[14] MATLAB® Ver 5.3, The Mathworks, Inc. 1999.

[15] CIRA 1965: COSPAR International Reference Atmosphere 1965, Amsterdam: North Holland Publishing Company, 1965, 306.

[16] Ibid, 109.

[17] King-Hele, 24.

[18] Vallado, 505.

Appendix A: Glossary

Argument of Periapsis: The angle measured between the line of nodes and the eccentricity vector.

Ballistic Coefficient: A term used in aerodynamics defined as the mass divided by the product of the coefficient of drag and the cross sectional area $\left(\frac{m}{C_D * A}\right)$.

Circular Error Probable: The radius of a circle where 50% of the computed positions will lie within the circle.

Circular Orbit: An orbit where the eccentricity of the orbit is equal to zero.

Coefficient of Drag: A dimensionless value which reflects the satellite's susceptibility to drag. forces.[1] (C_D)

Direct Orbit: An orbit with an inclination less than 90°.

Earth's Gravitational Parameter: The term that is defined by the product of the gravitational constant and the Earth's mass $(m = G * m_{\oplus})$.

Eccentricity: The parameter of an ellipse defining the shape of the orbit, which is the ratio of the distance between the two foci to the major axis (2a).

Eccentricity vector: A vector that points in the direction of periapsis and has the magnitude of the eccentricity.

Eccentric Orbit: An orbit with an eccentricity between 0 and 1. An eccentricity of 0 defines a circular orbit while an eccentricity of 1 defines a parabolic orbit.

Flight path angle: The angle between the velocity vector and the local horizon, where the local horizon is perpendicular to the position vector.

Inclination: The angle between an orbit's angular momentum vector and the Earth's angular momentum vector. It can also be measured by the angle between the orbital plane and the Earth's equatorial plane.

Line of nodes: The vector connecting the center of the Earth to the ascending node. The ascending node is the point where the satellite crosses the equatorial plane.

Longitude of Ascending node: The angle between the $\hat{I}$ unit vector (in the Geocentric Equatorial coordinate system) and the line of nodes, where the $\hat{I}$ vector points in the direction of

[1] Vallado, 498.

the first point of Aries. The first point of Aries is defined by the line from the Earth to the Sun, when the Earth is at the vernal equinox.

Low-Earth Orbit: An orbit with altitudes below 800 km.

Mean Motion: The mean angular rate of a satellite's orbit defined by $n \equiv \sqrt{\frac{m}{a^3}}$.

Periapsis: The point of the satellite's orbit that is the closest to the central body.

Perigee: The point of the satellite's orbit that is the closest to the Earth.

Polar Orbit: An orbit with an inclination of 90°.

Retrograde orbit: An orbit with inclinations greater than 90°.

Scale Height: The distance where the atmospheric density decreases by a factor of $\frac{1}{e}$.

Semimajor Axis: Half of the distance of the ellipse's length.

True Anomaly: The angle between the eccentricity vector and the position vector as shown in Figure 1 on page 11.

Appendix B: Additional Results – Density / Error Plots

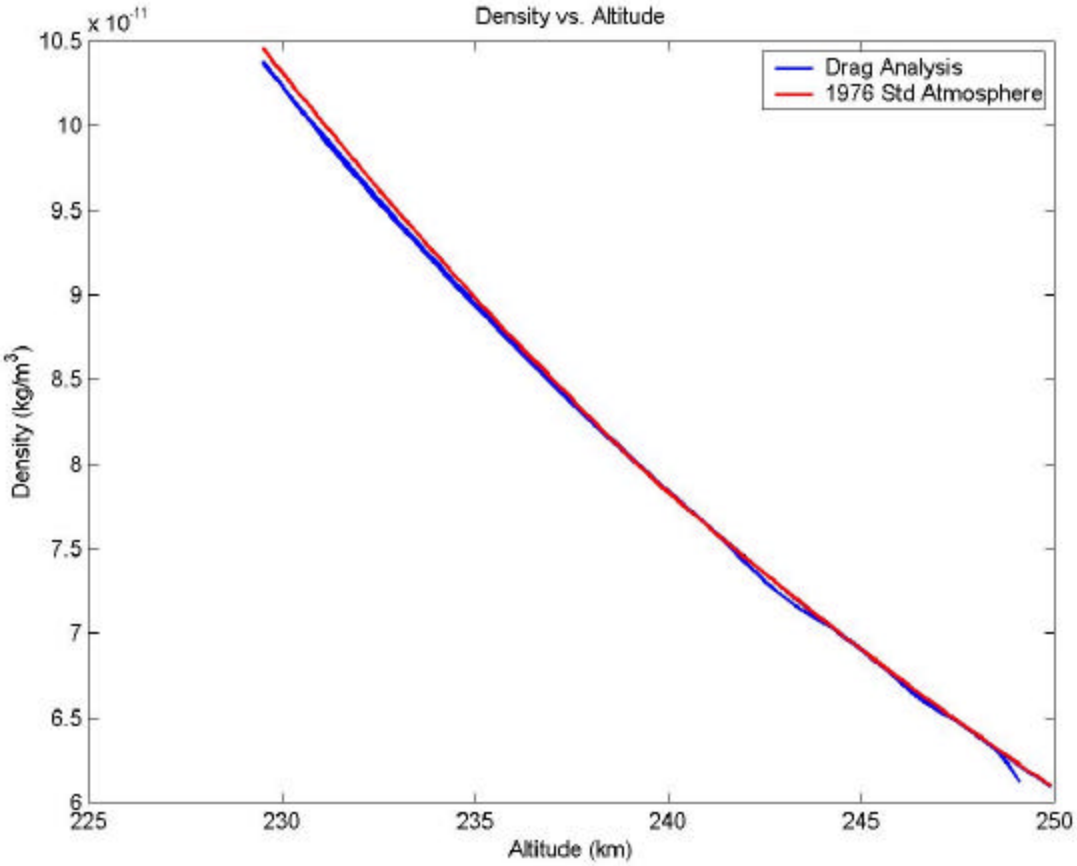

Figure B.1 Density vs. Altitude For an Orbit Defined By:
a = 6628 km
e = 0
i = 0°

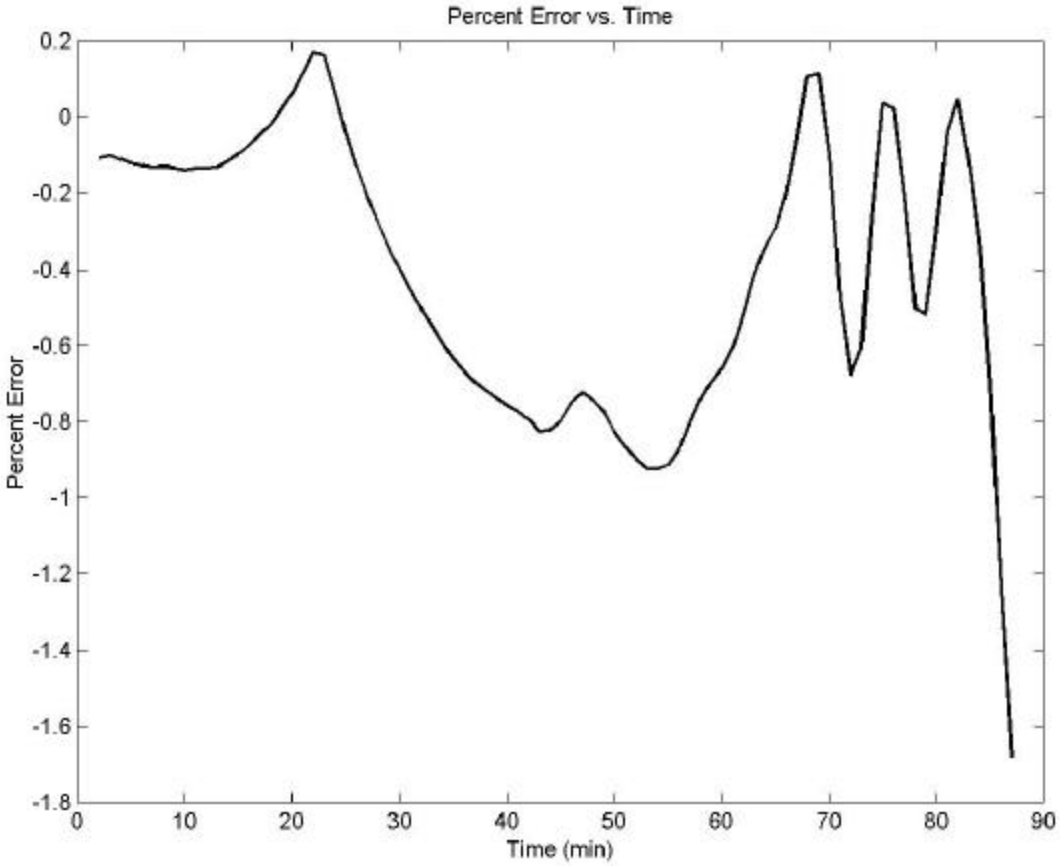

Figure B.2 Percent Error vs. Time For an Orbit Defined By:
a = 6628 km
e = 0
i = 0°

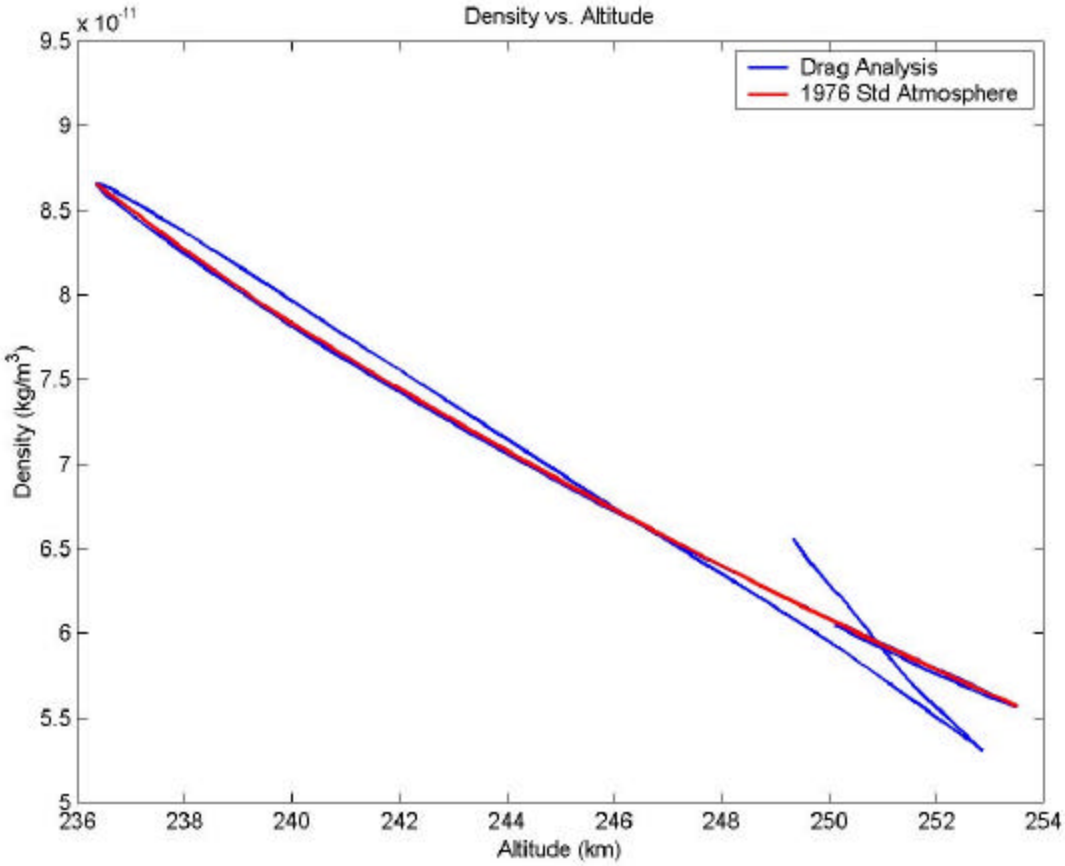

Figure B.3 Density vs. Altitude For an Orbit Defined By:
a = 6628 km
e = 0
i = 45°

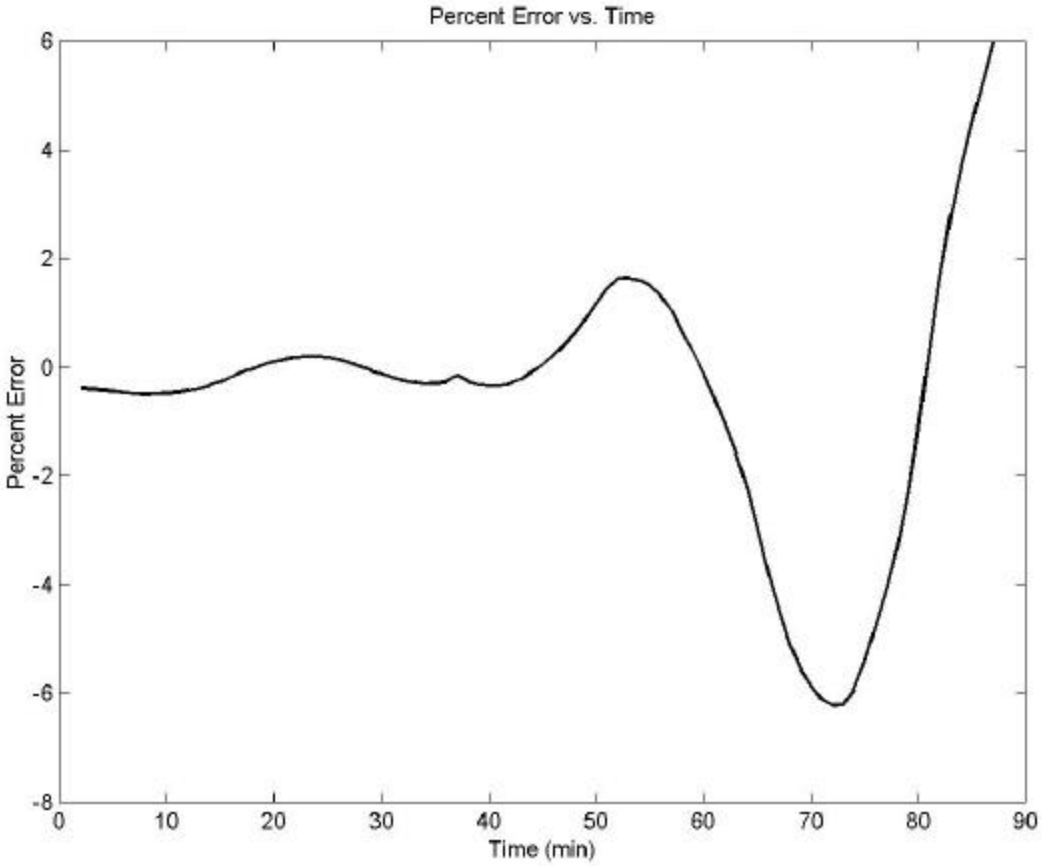

Figure B.4 Percent Error vs. Time For an Orbit Defined By:
a = 6628 km
e = 0
i = 45°

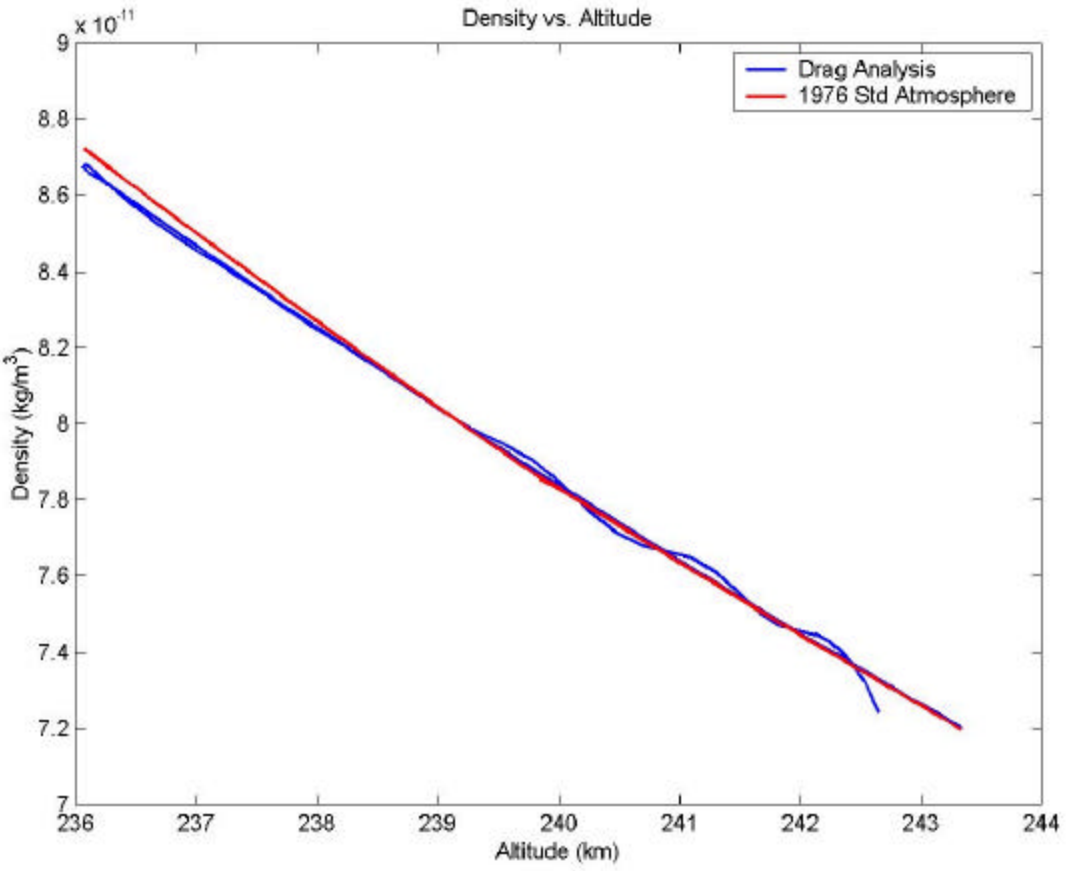

Figure B.5 Density vs. Altitude For an Orbit Defined By:

a = 6628 km
e = 0.001
i = 0°

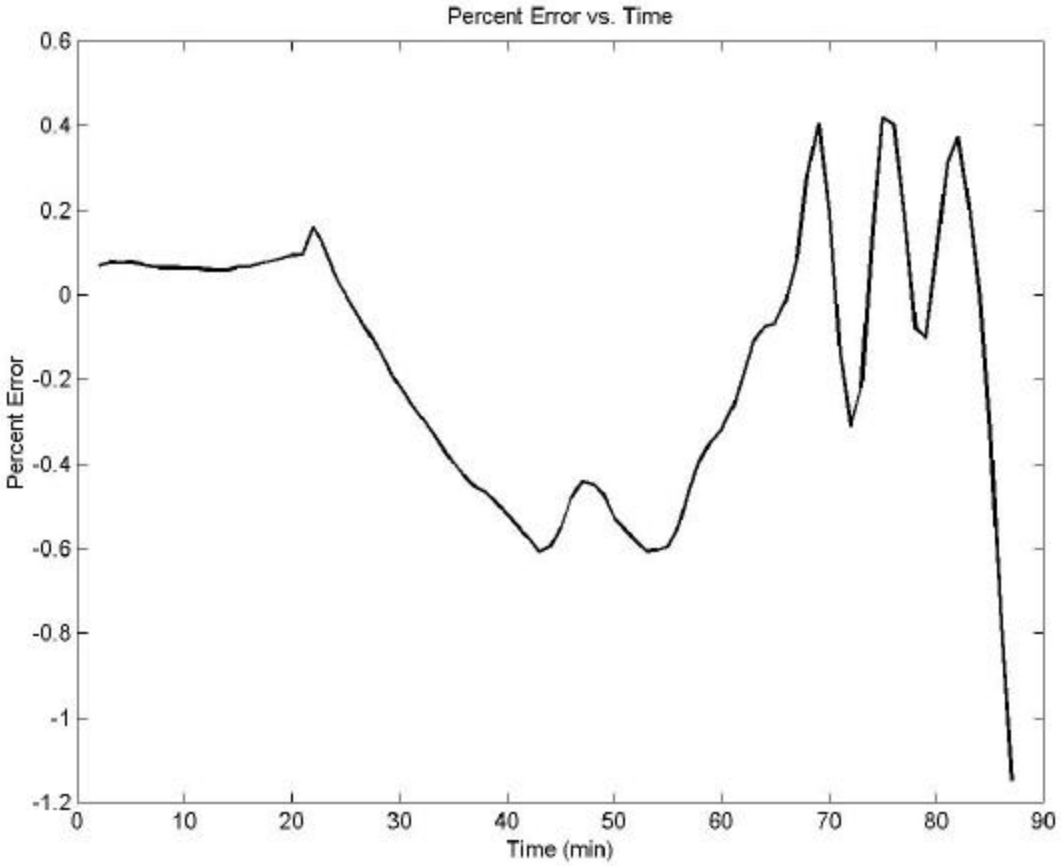

Figure B.6 Percent Error vs. Time For an Orbit Defined By:
a = 6628 km
e = 0.001
i = 0°

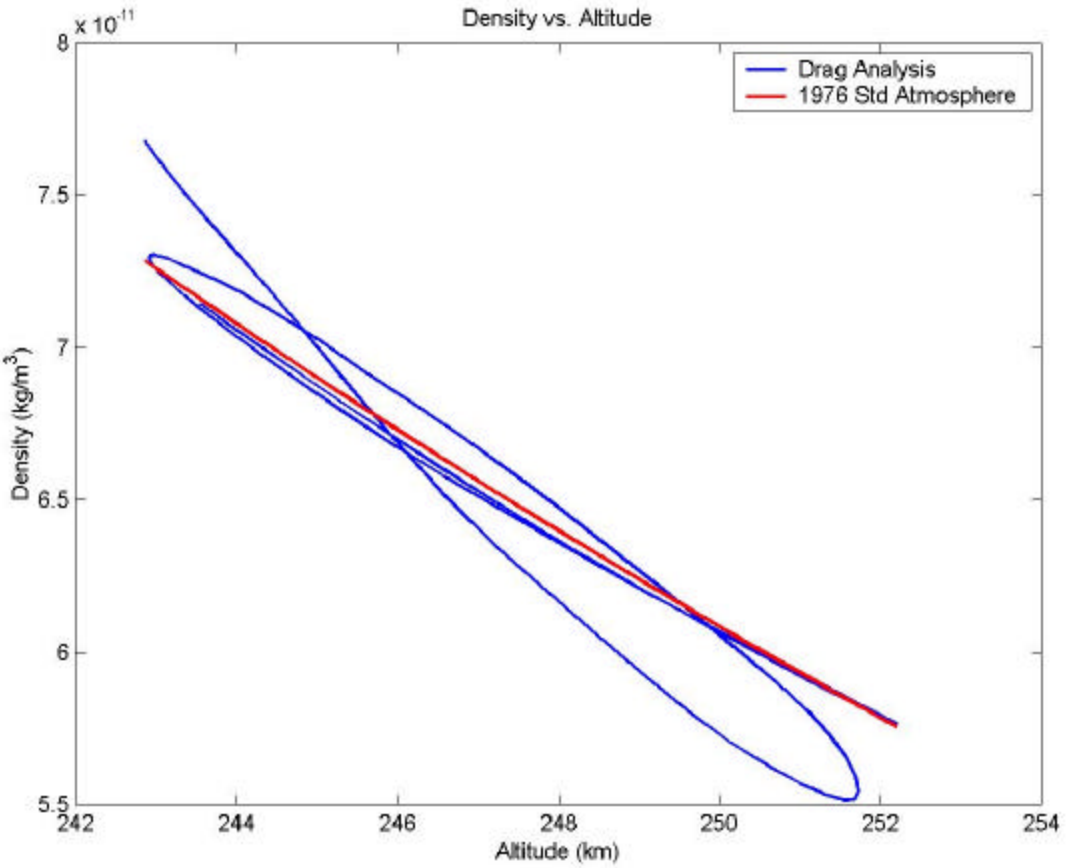

Figure B.7 Density vs. Altitude For an Orbit Defined By:
a = 6628 km
e = 0.001
i = 45°

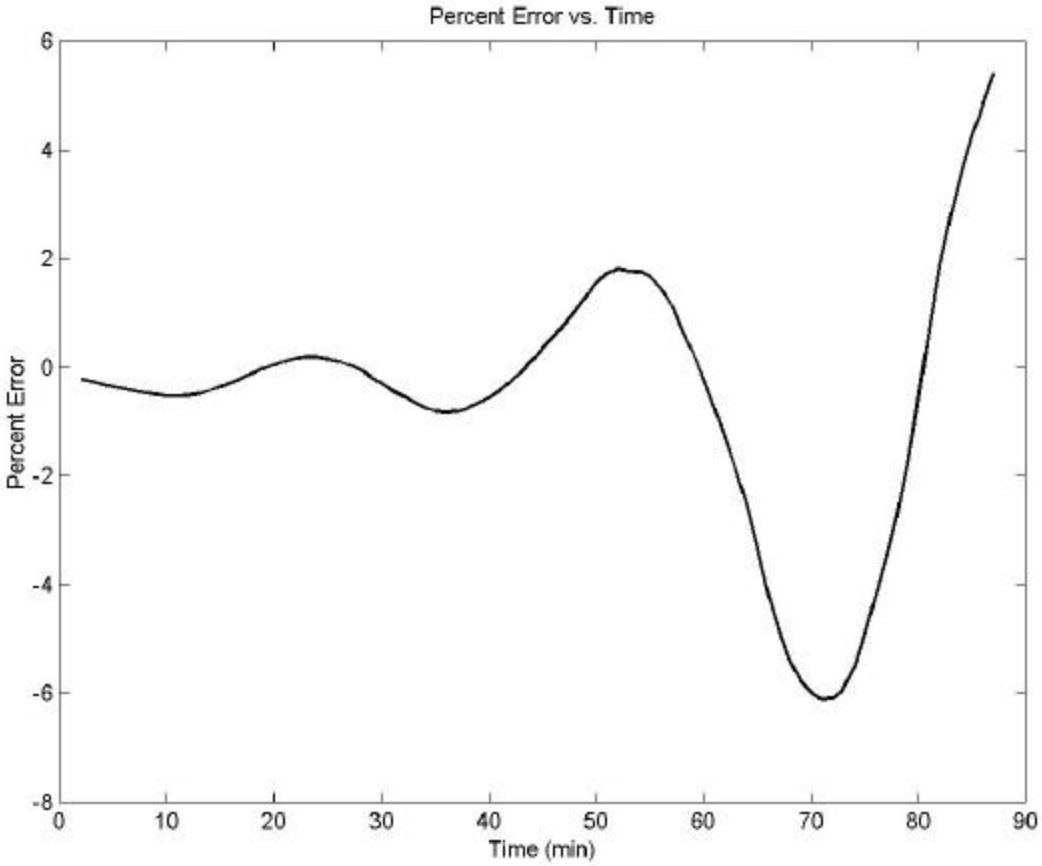

Figure B.8 Percent Error vs. Time For an Orbit Defined By:
a = 6628 km
e = 0.001
i = 45°

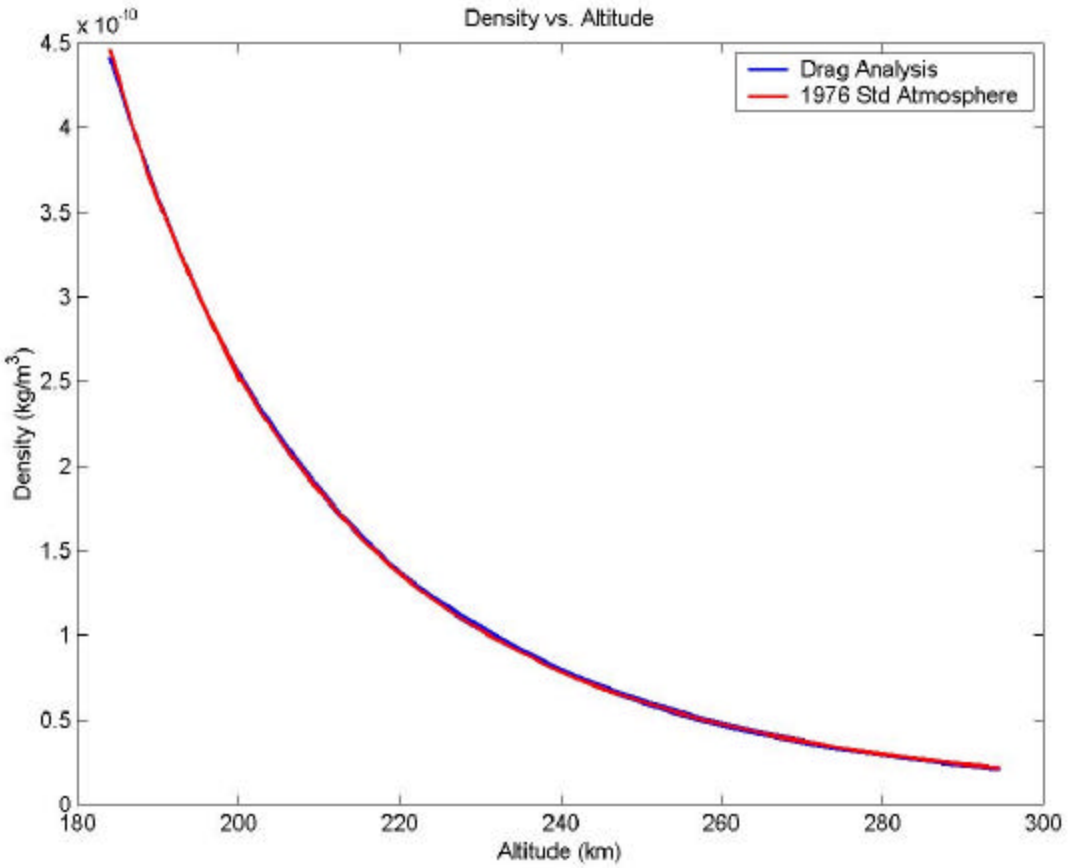

Figure B.9 Density vs. Altitude For an Orbit Defined By:
a = 6628 km
e = 0.01
i = 0°

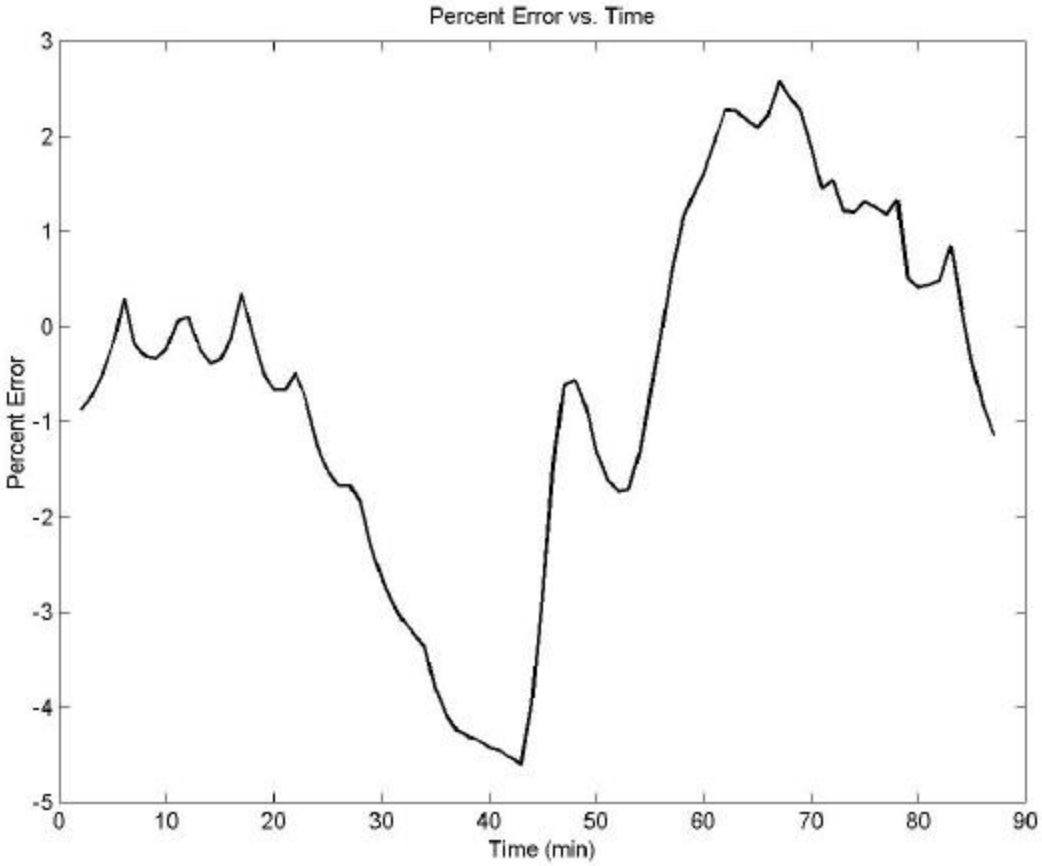

Figure B.10 Percent Error vs. Time For an Orbit Defined By:
a = 6628 km
e = 0.01
i = 0°

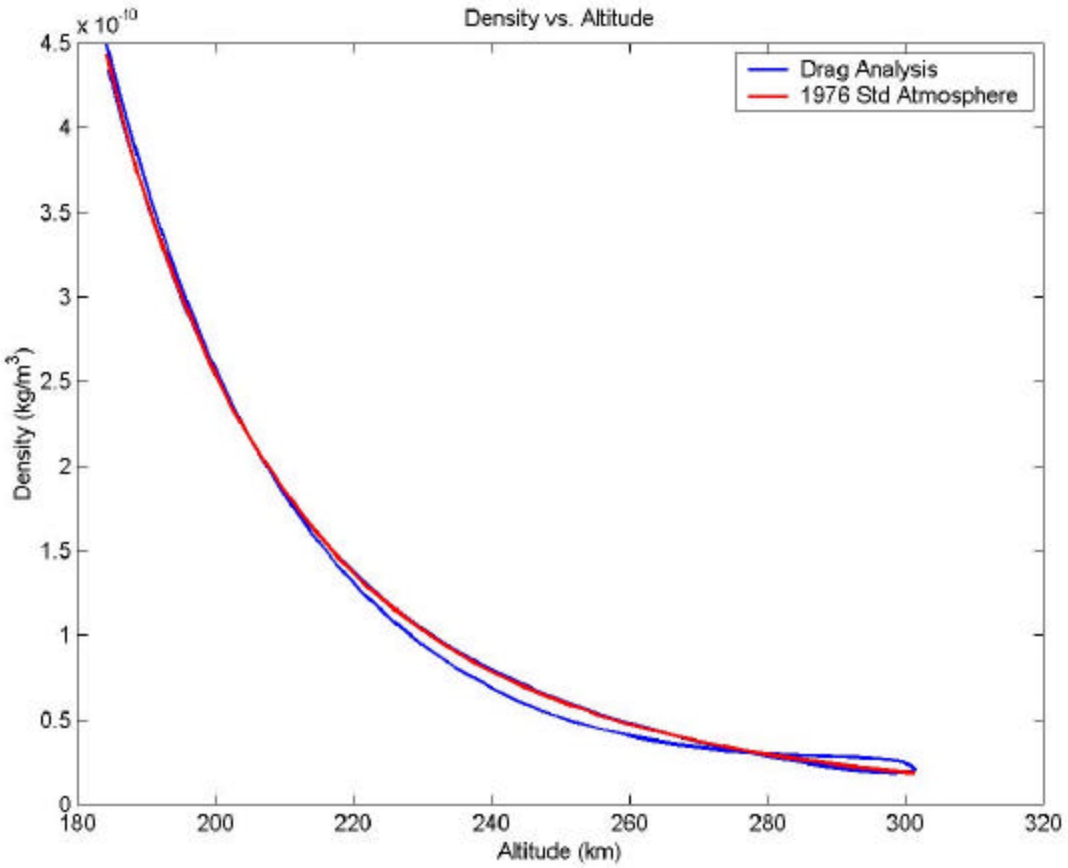

Figure B.11 Density vs. Altitude For an Orbit Defined By:
a = 6628 km
e = 0.01
i = 45°

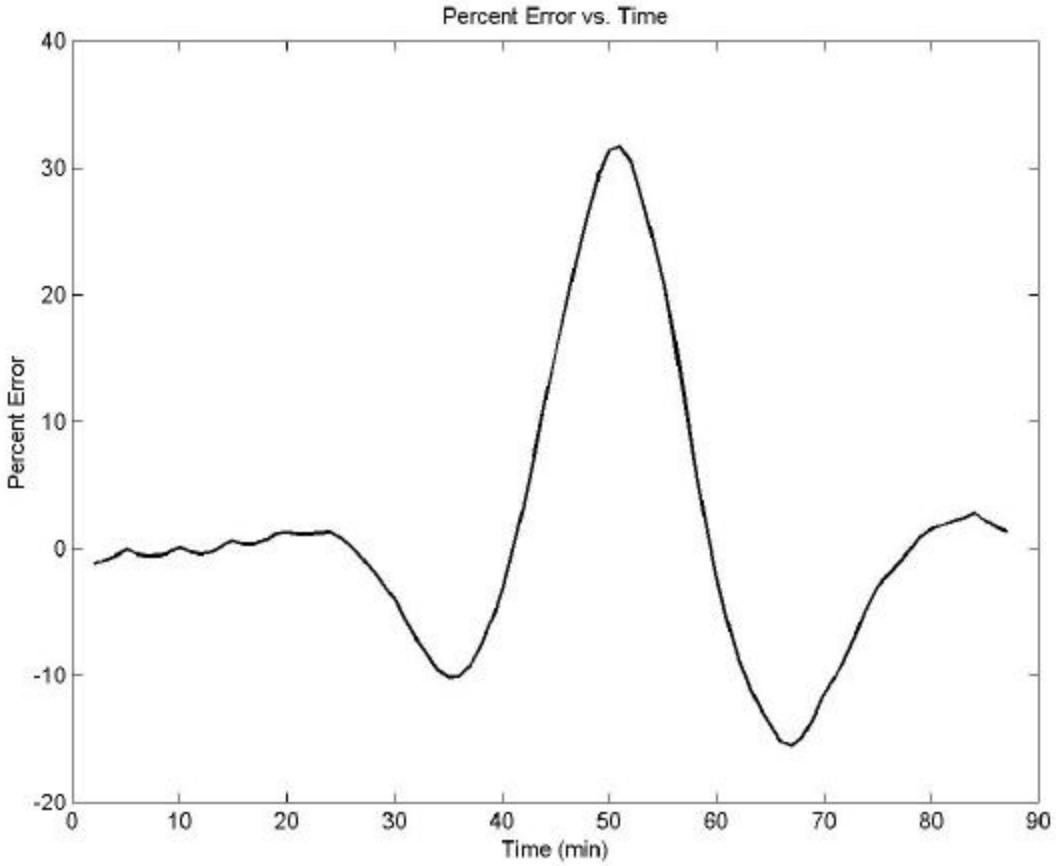

Figure B.12 Percent Error vs. Time For an Orbit Defined By:
a = 6628 km
e = 0.01
i = 45°

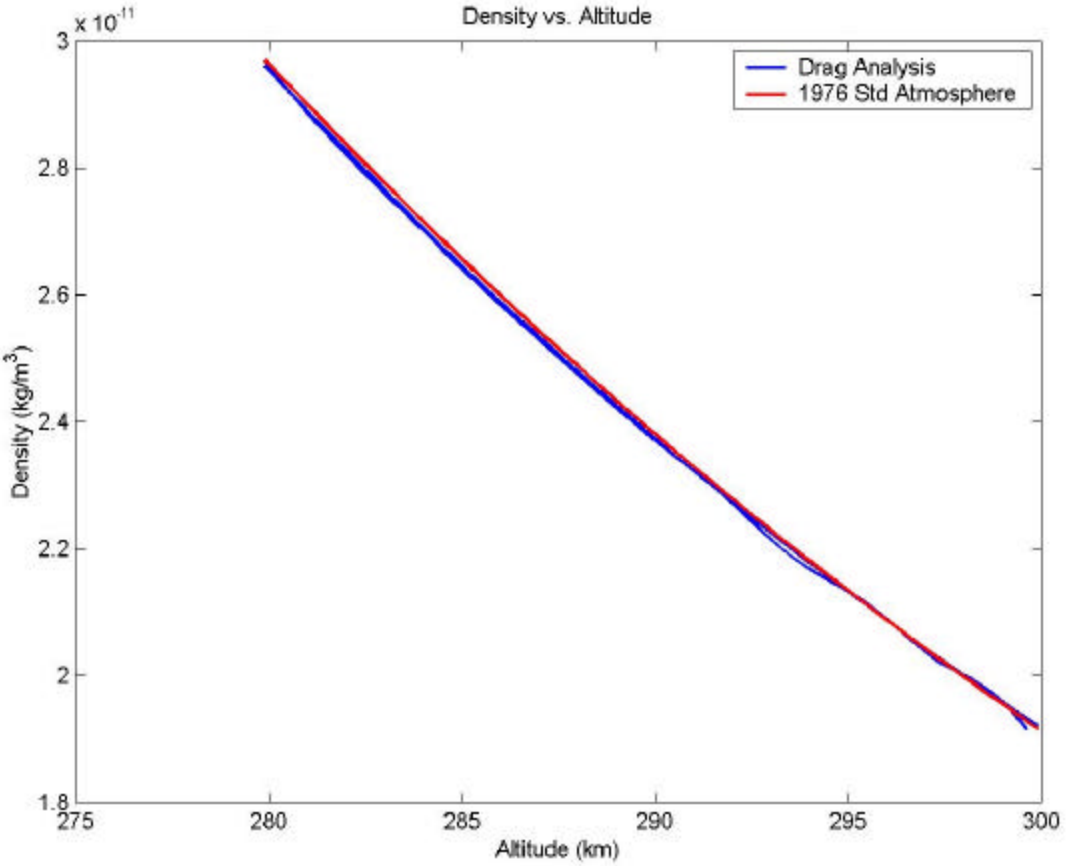

Figure B.13 Density vs. Altitude For an Orbit Defined By:
a = 6678 km
e = 0
i = 0°

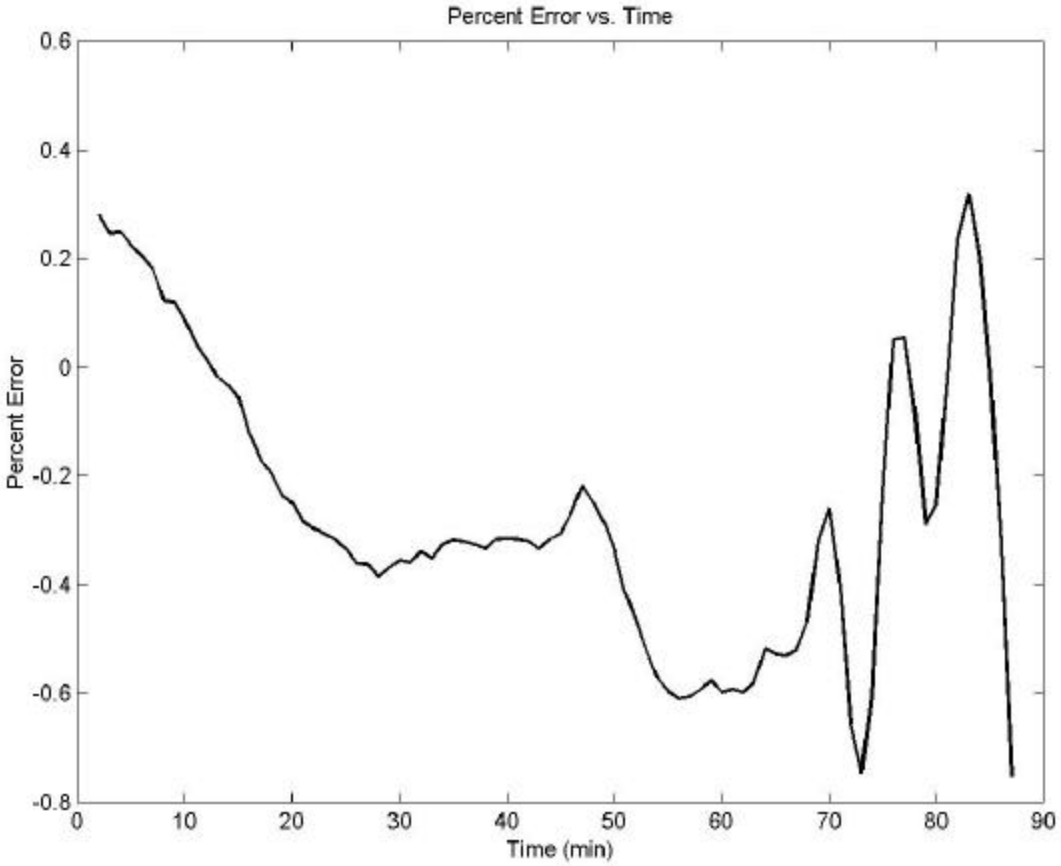

Figure B.14 Density vs. Altitude For an Orbit Defined By:
a = 6678 km
e = 0
i = 0°

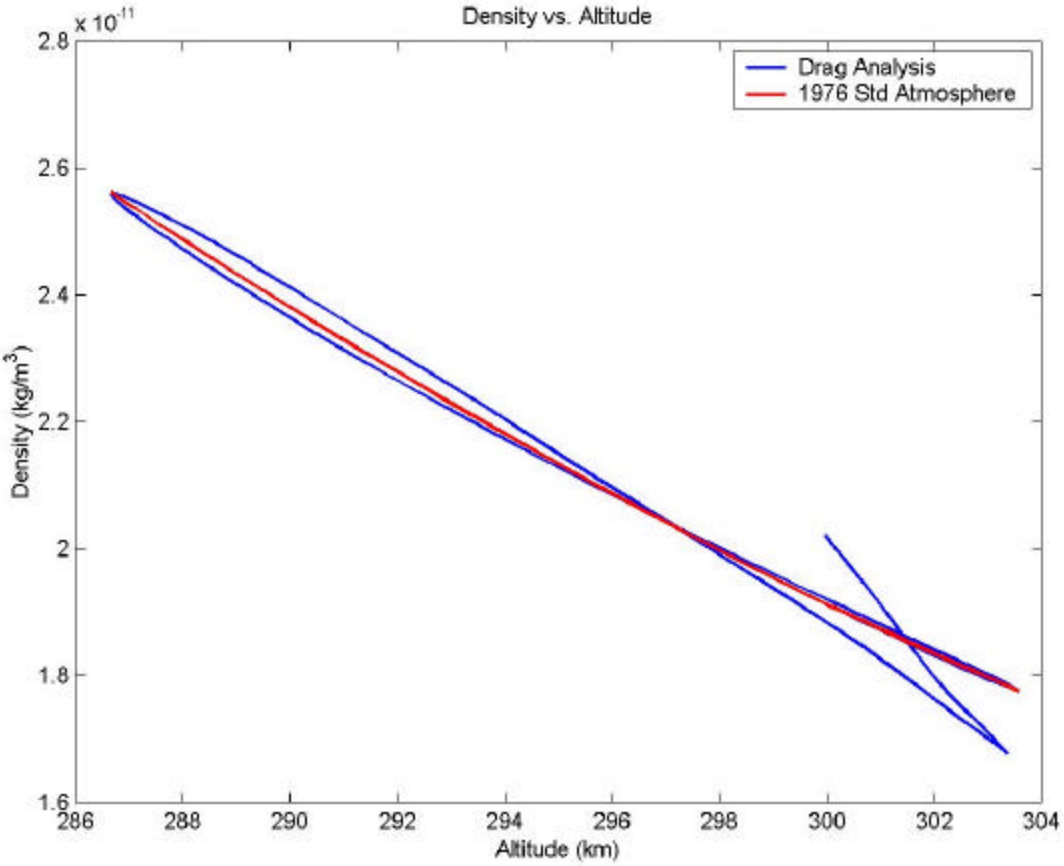

Figure B.15 Density vs. Altitude For an Orbit Defined By:
a = 6678 km
e = 0
i = 45°

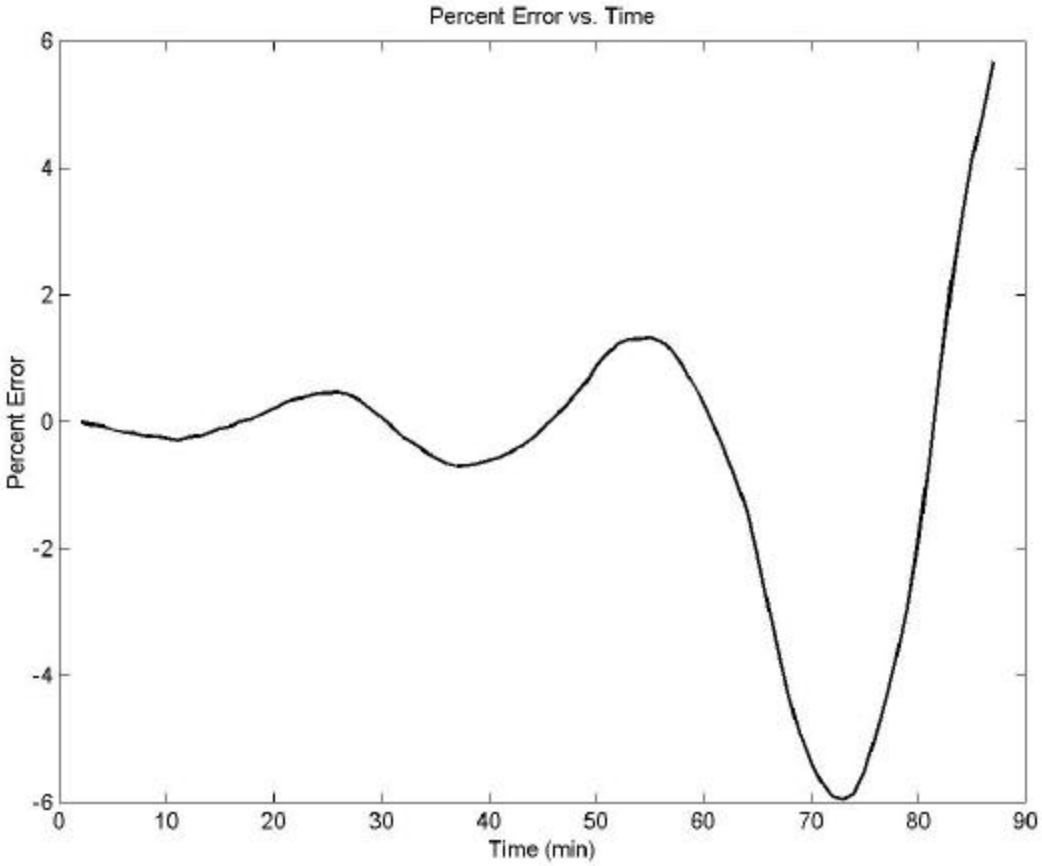

Figure B.16 Density vs. Altitude For an Orbit Defined By:
a = 6678 km
e = 0
i = 45°

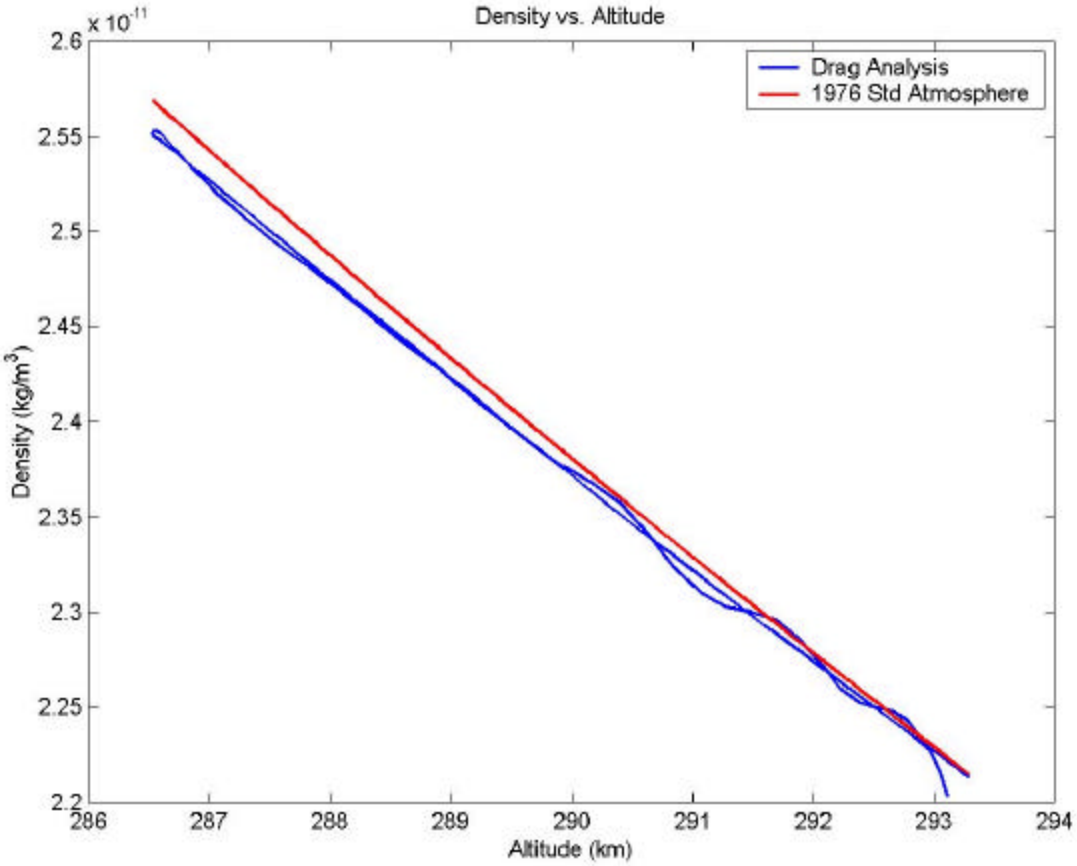

Figure B.17 Density vs. Altitude For an Orbit Defined By:
a = 6678 km
e = 0.001
i = 0°

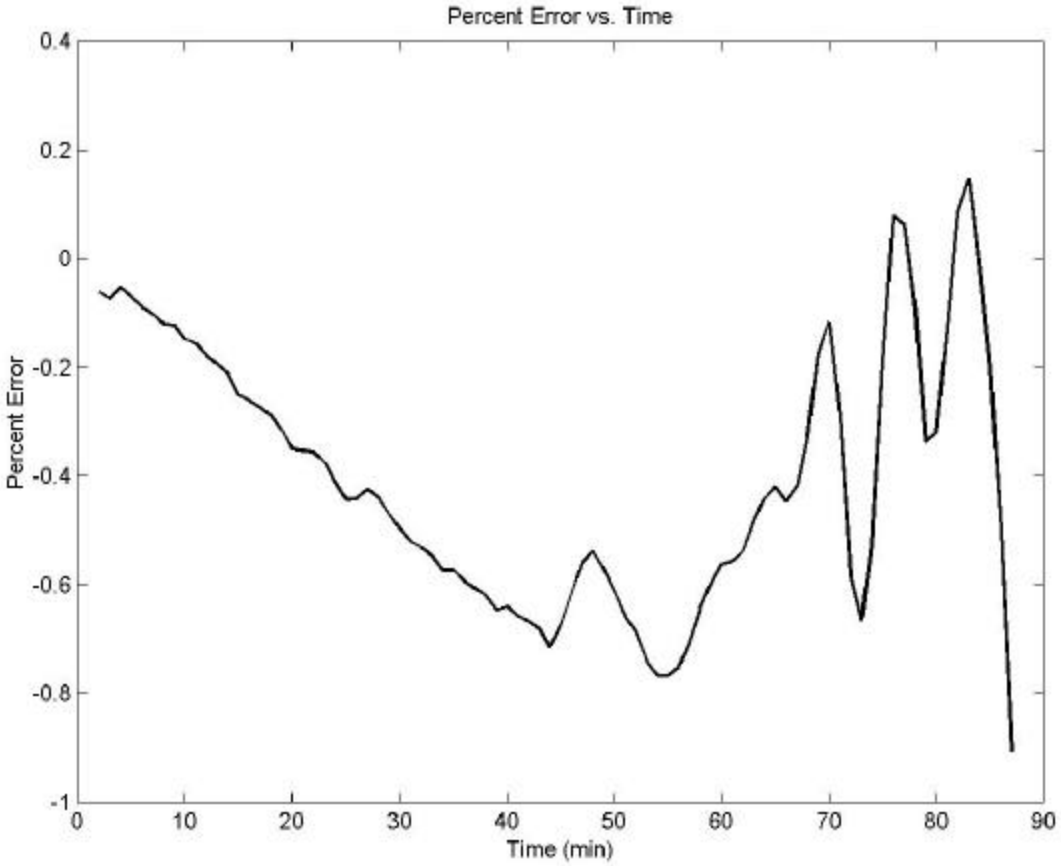

Figure B.18 Percent Error vs. Time For an Orbit Defined By:
a = 6678 km
e = 0.001
i = 0°

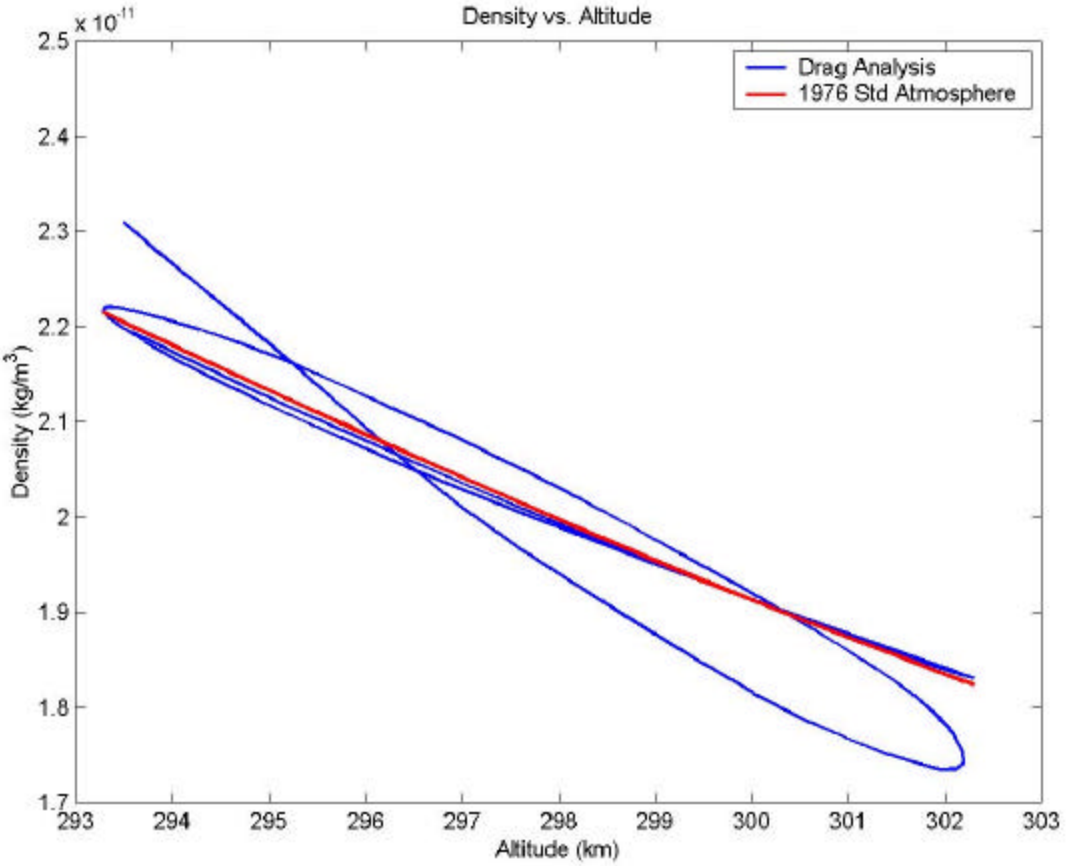

Figure B.19 Density vs. Altitude For an Orbit Defined By:
a = 6678 km
e = 0.001
i = 45°

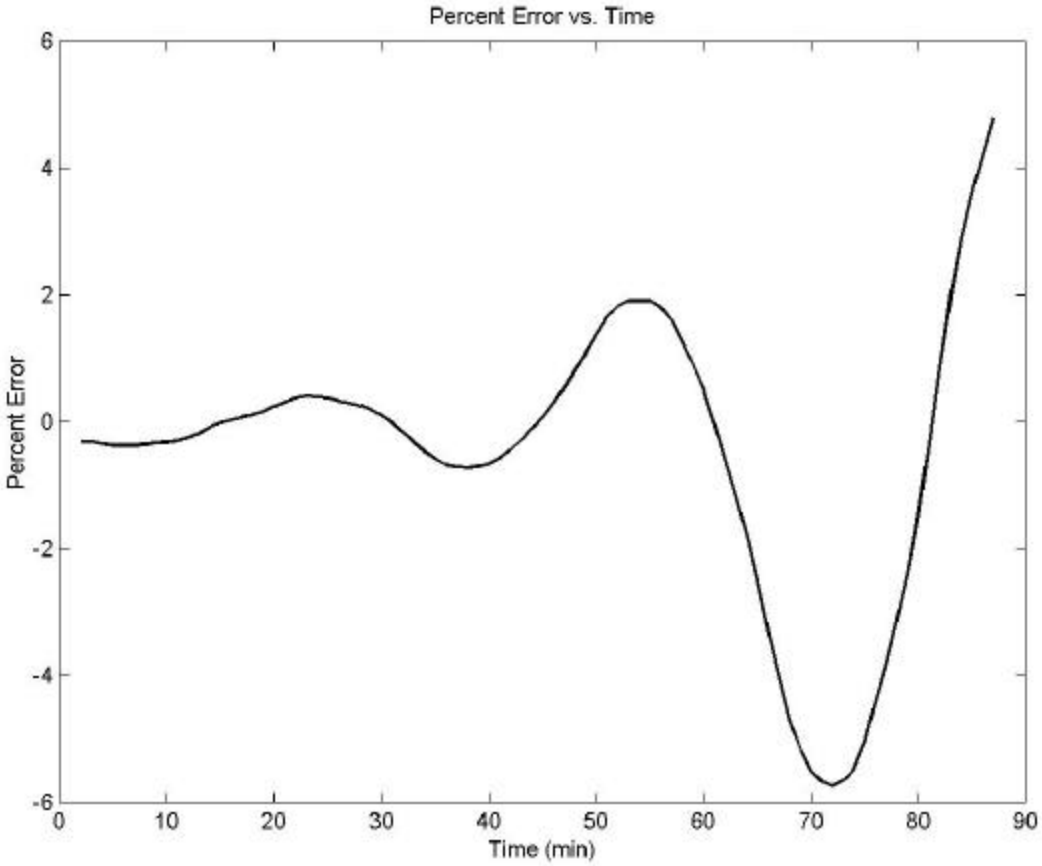

Figure B.20 Percent Error vs. Time For an Orbit Defined By:
a = 6678 km
e = 0.001
i = 45°

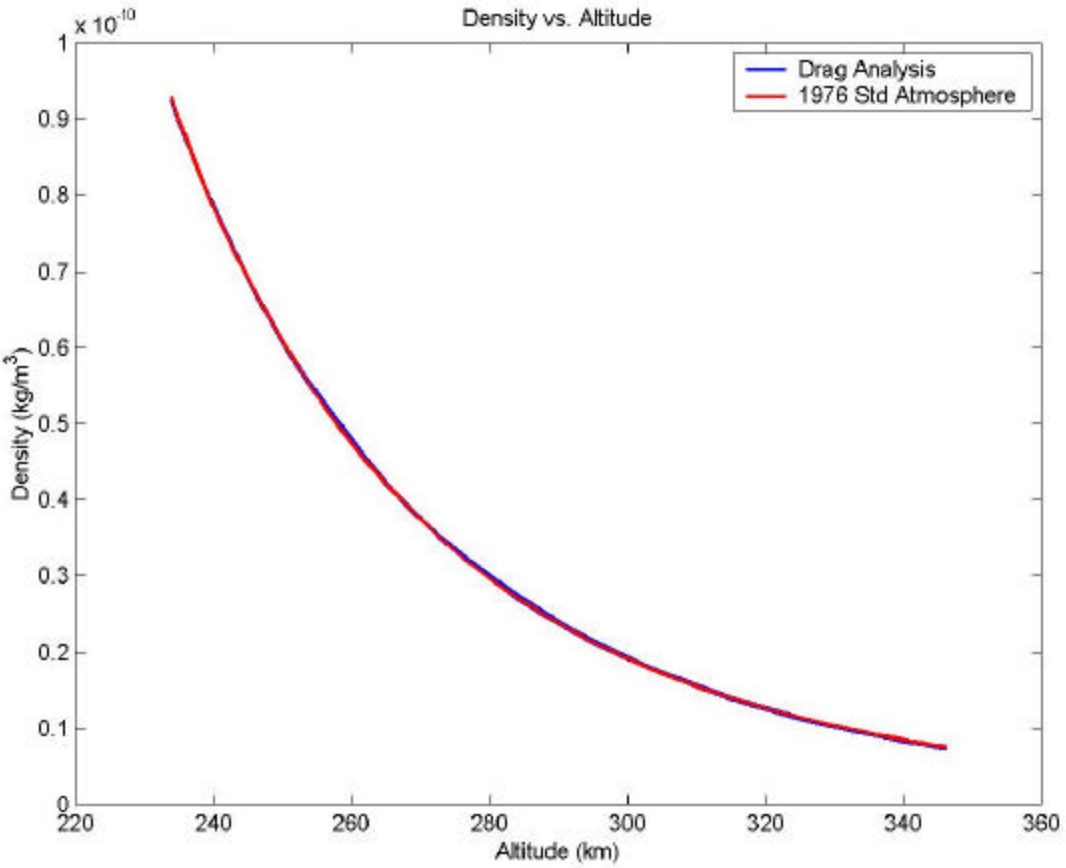

Figure B.21 Density vs. Altitude For an Orbit Defined By:
a = 6678 km
e = 0.01
i = 0°

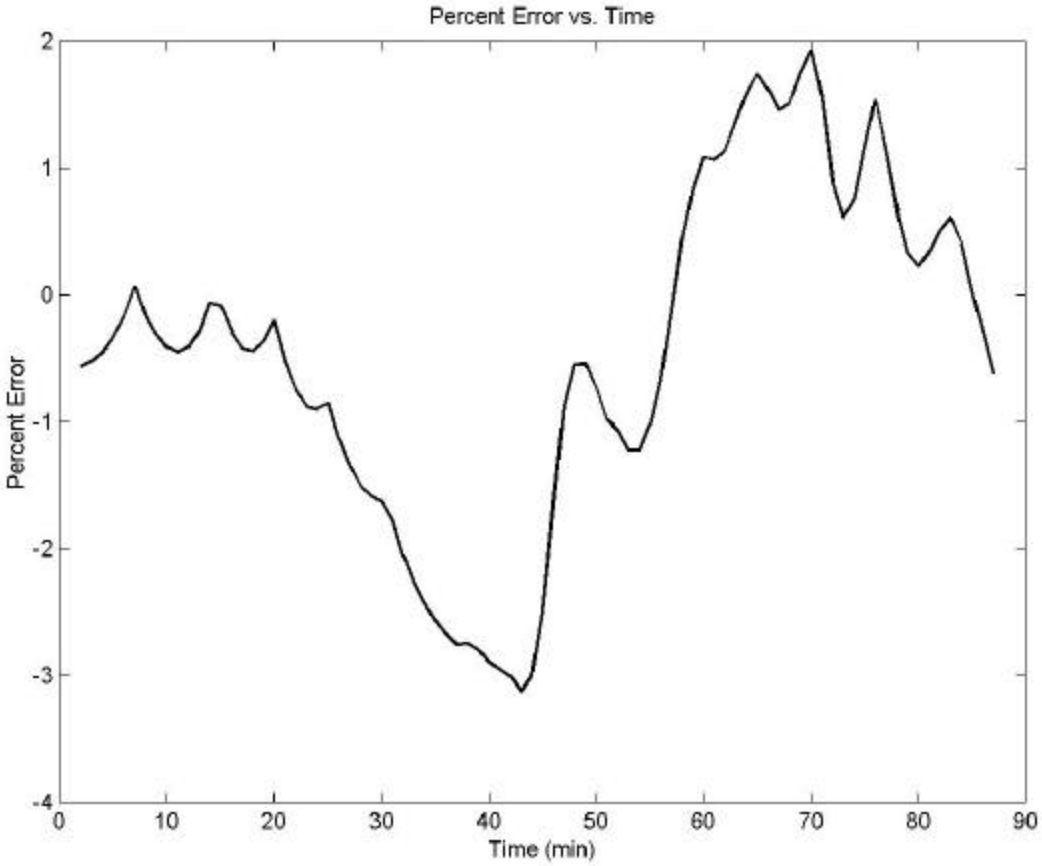

Figure B.22 Percent Error vs. Time For an Orbit Defined By:
a = 6678 km
e = 0.01
i = 0°

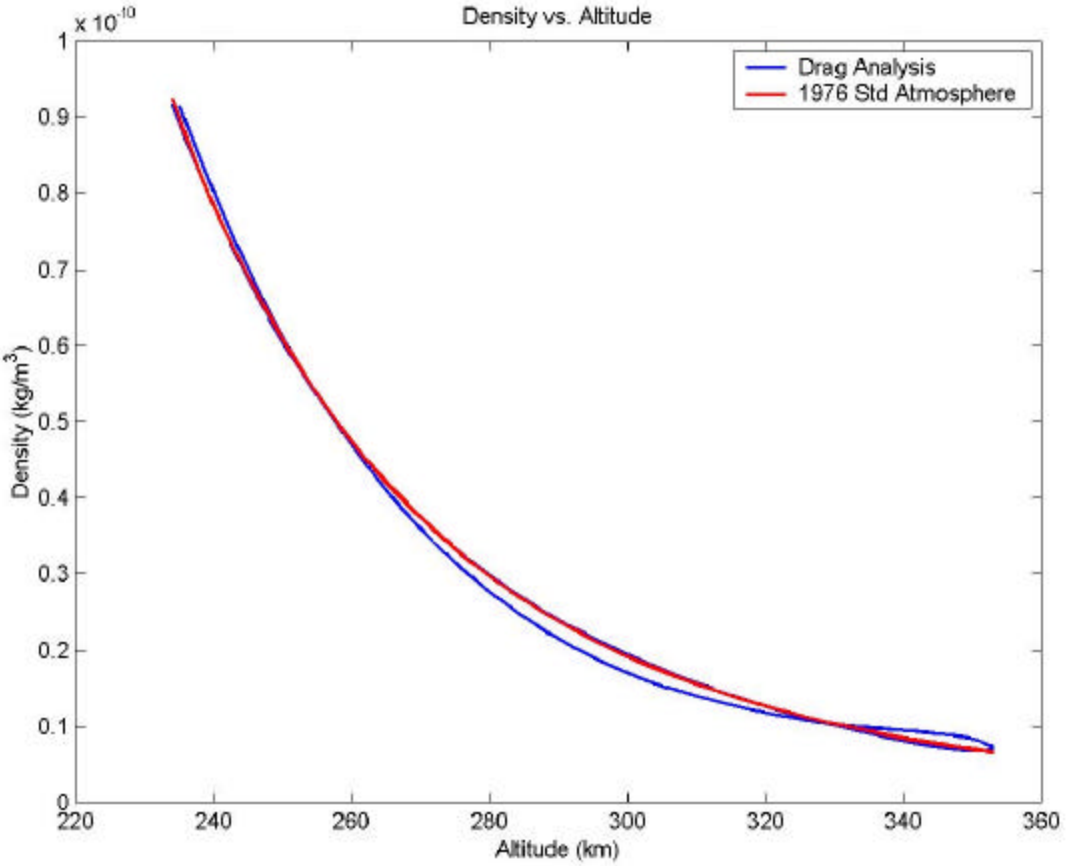

Figure B.23 Density vs. Altitude For an Orbit Defined By:
a = 6678 km
e = 0.01
i = 45°

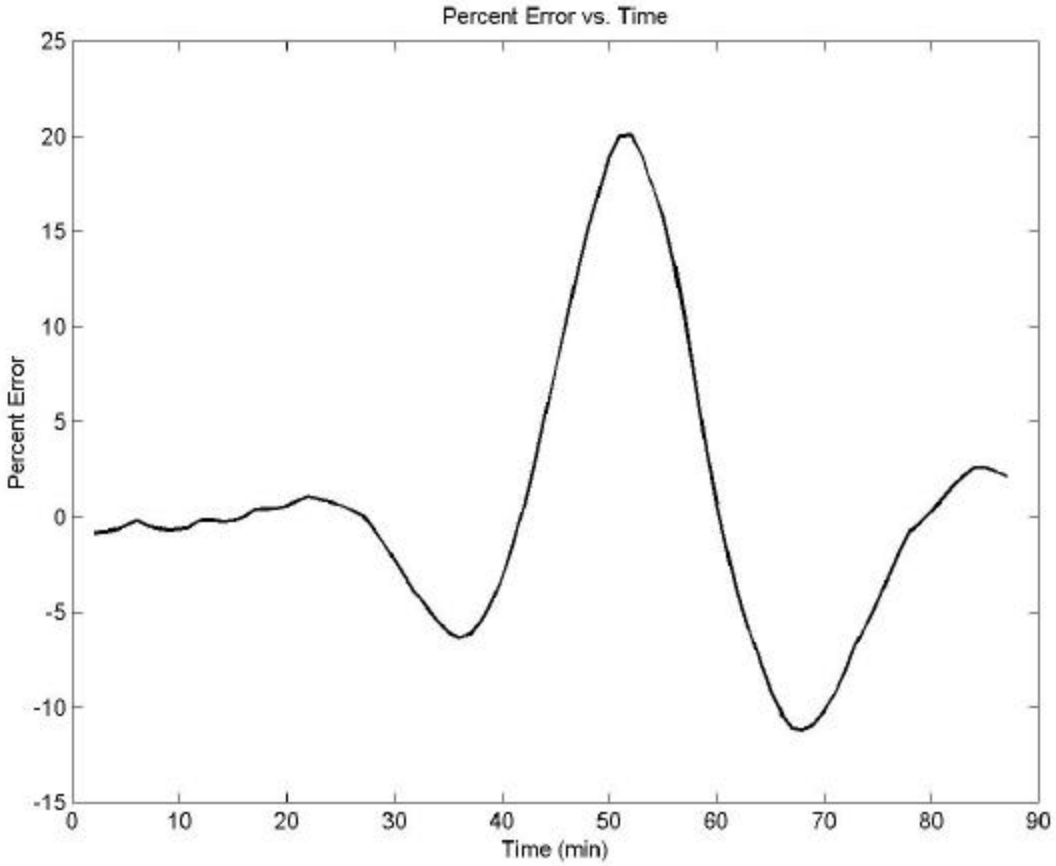

Figure B.24 Density vs. Altitude For an Orbit Defined By:
a = 6678 km
e = 0.01
i = 45°

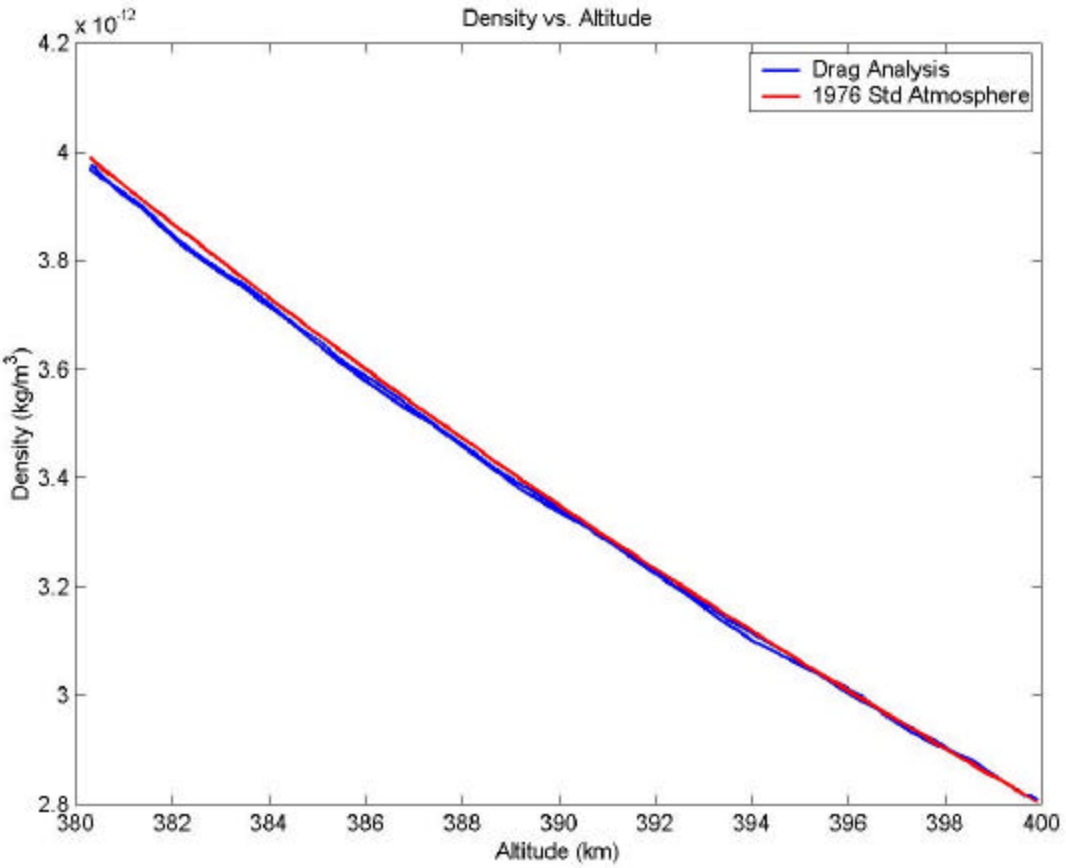

Figure B.25 Density vs. Altitude For an Orbit Defined By:
a = 6778 km
e = 0
i = 0°

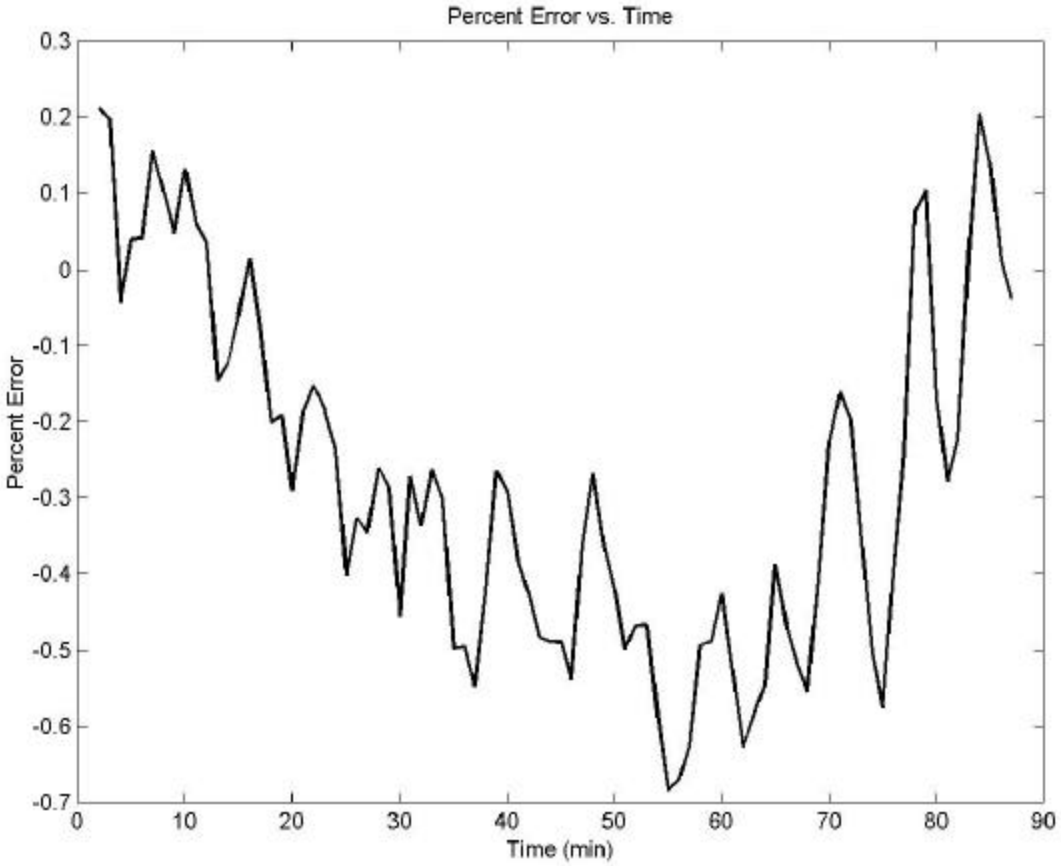

Figure B.26 Percent Error vs. Time For an Orbit Defined By:
a = 6778 km
e = 0
i = 0°

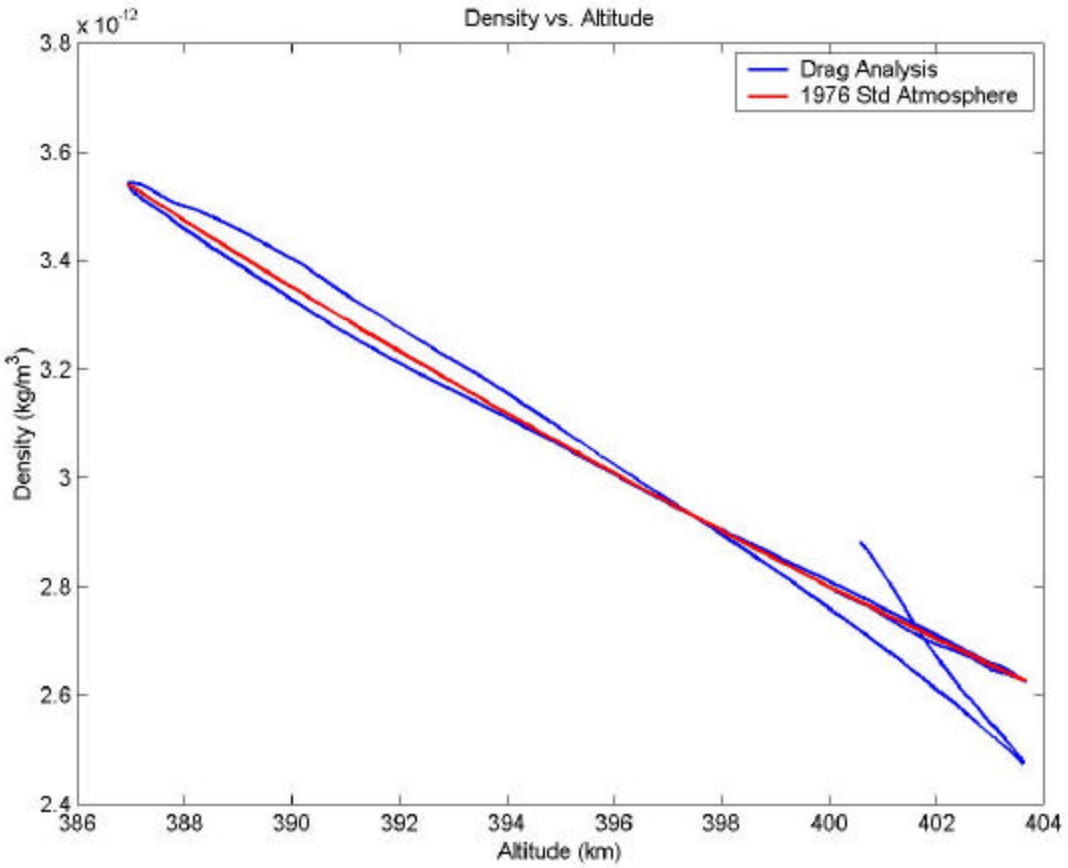

Figure B.27 Density vs. Altitude For an Orbit Defined By:
a = 6778 km
e = 0
i = 45°

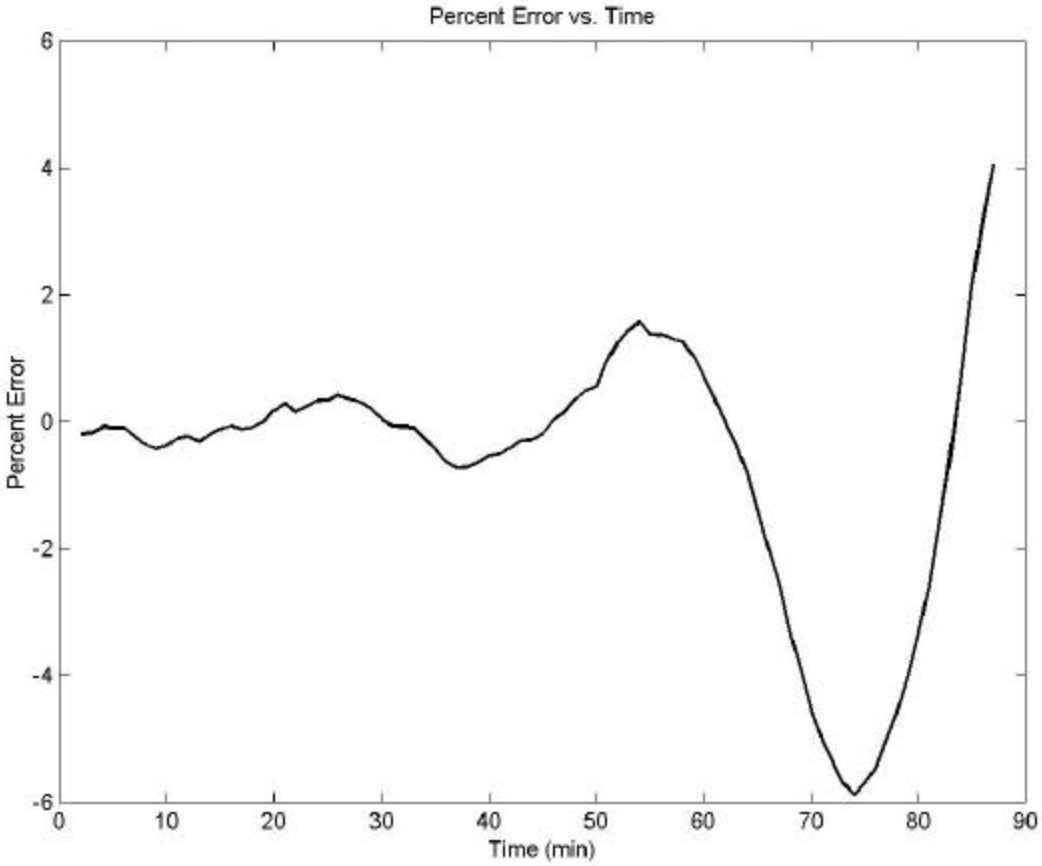

Figure B.28 Percent Error vs. Time For an Orbit Defined By:
a = 6778 km
e = 0
i = 45°

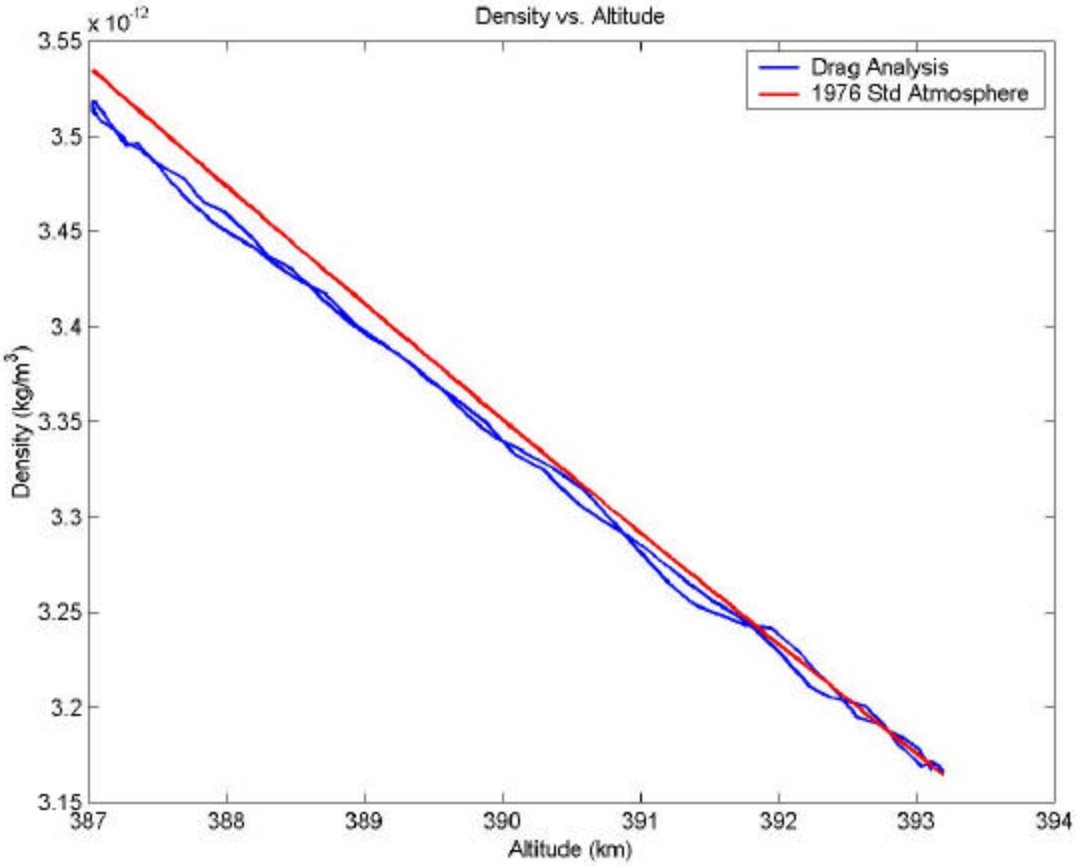

Figure B.29 Density vs. Altitude For an Orbit Defined By:
a = 6778 km
e = 0.001
i = 0°

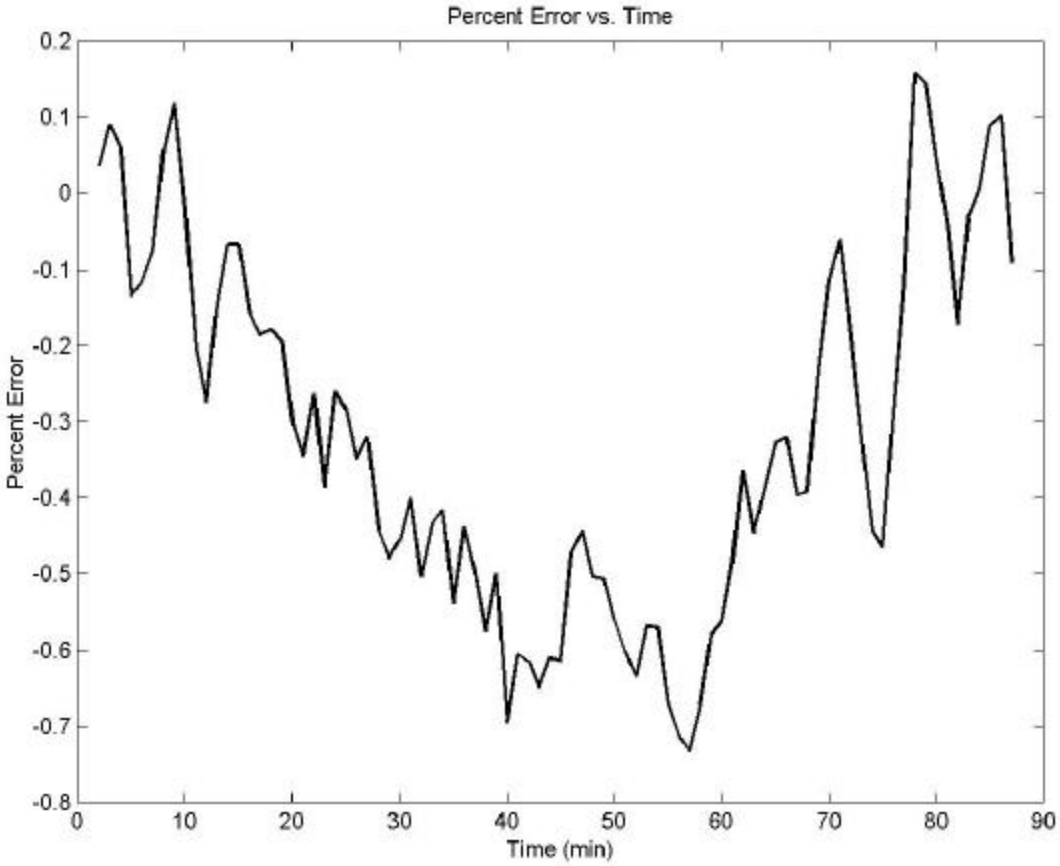

Figure B.30 Percent Error vs. Time For an Orbit Defined By:
a = 6778 km
e = 0.001
i = 0°

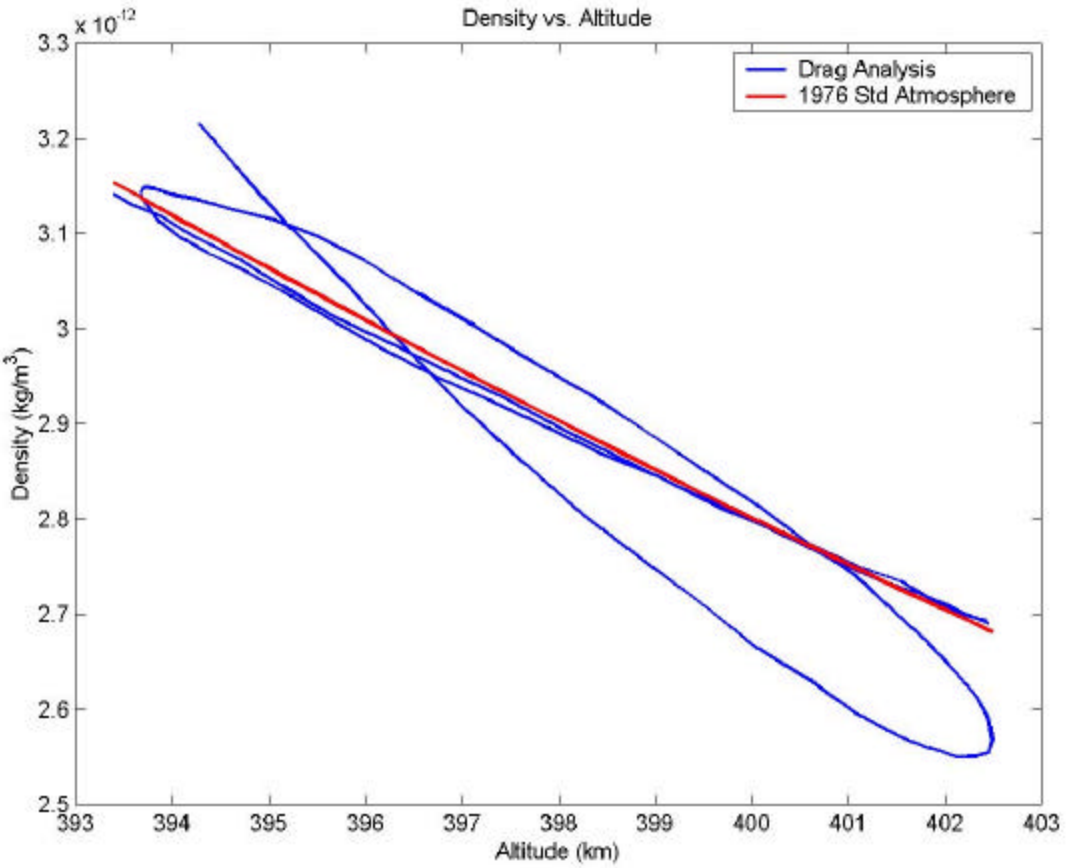

Figure B.31 Density vs. Altitude For an Orbit Defined By:
a = 6778 km
e = 0.001
i = 45°

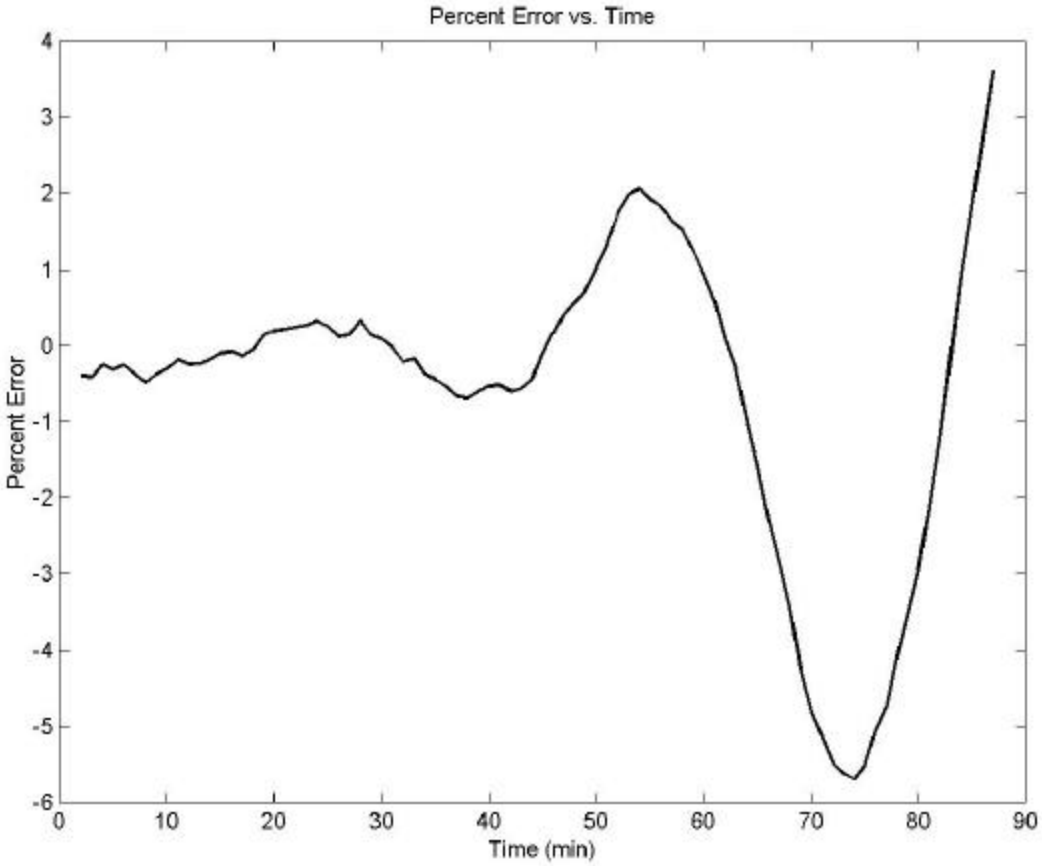

Figure B.32 Percent Error vs. Time For an Orbit Defined By:
a = 6778 km
e = 0.001
i = 45°

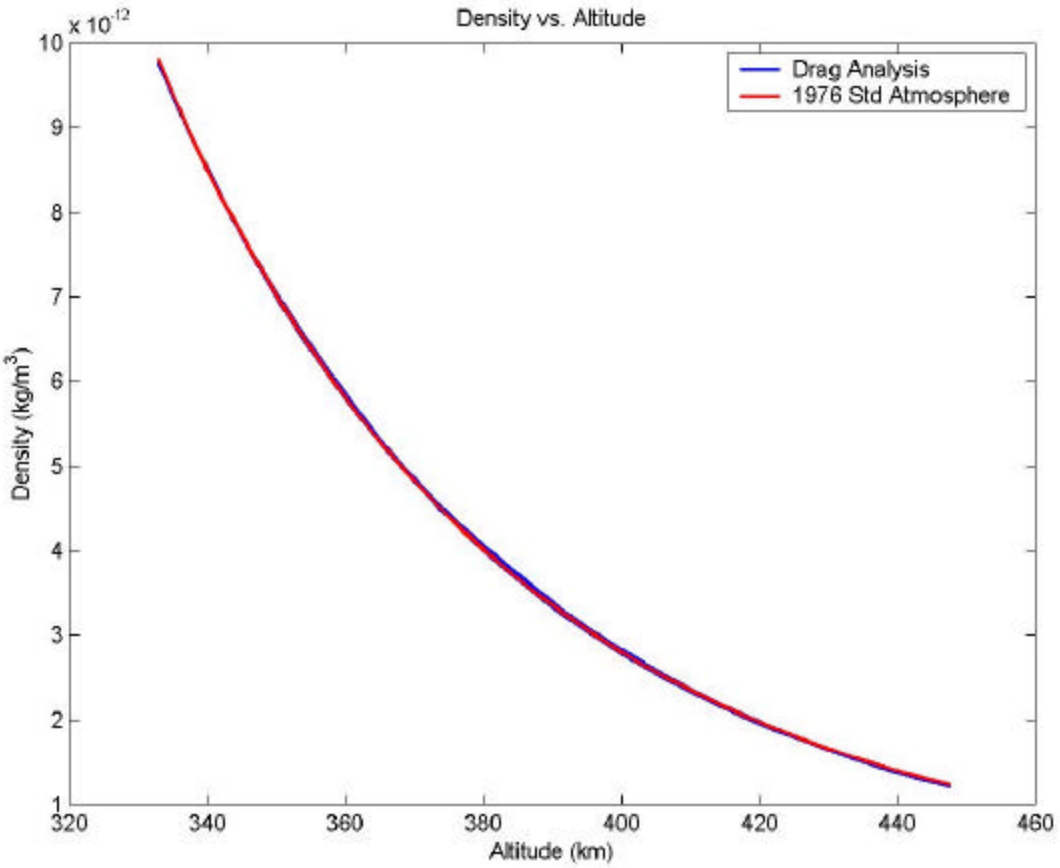

Figure B.33 Density vs. Altitude For an Orbit Defined By:
a = 6778 km
e = 0.01
i = 0°

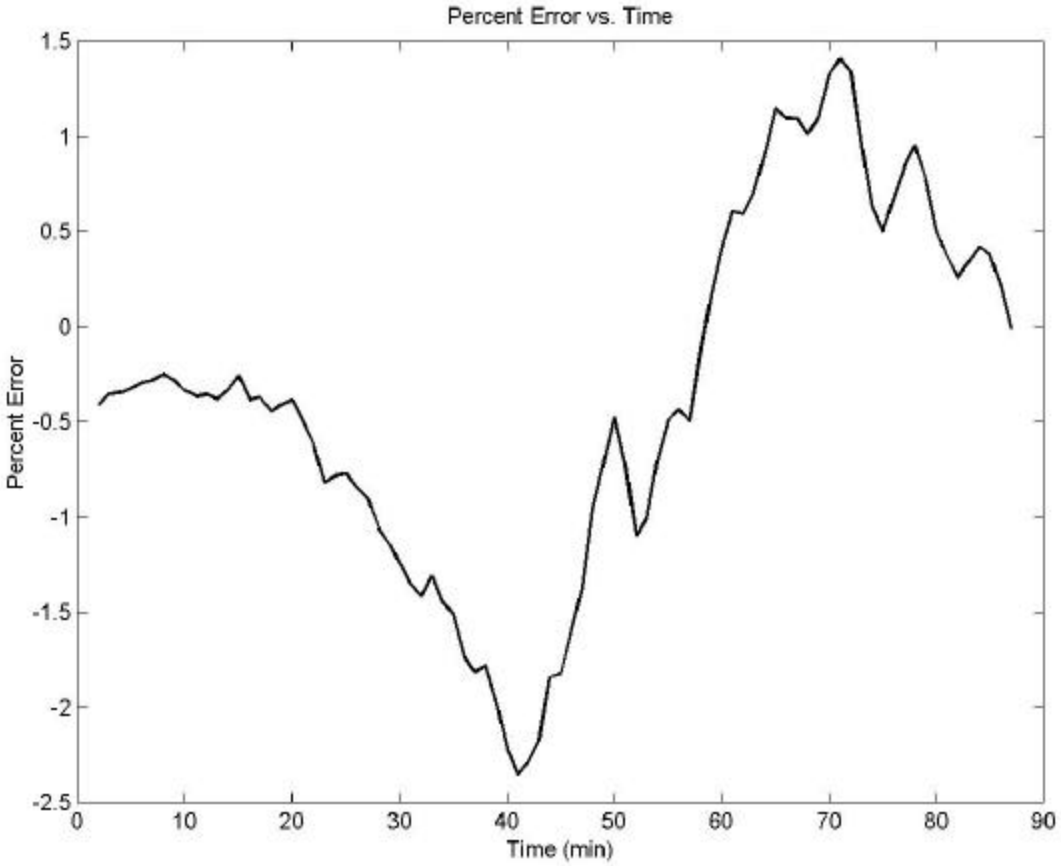

Figure B.34 Percent Error vs. Time For an Orbit Defined By:
a = 6778 km
e = 0.01
i = 0°

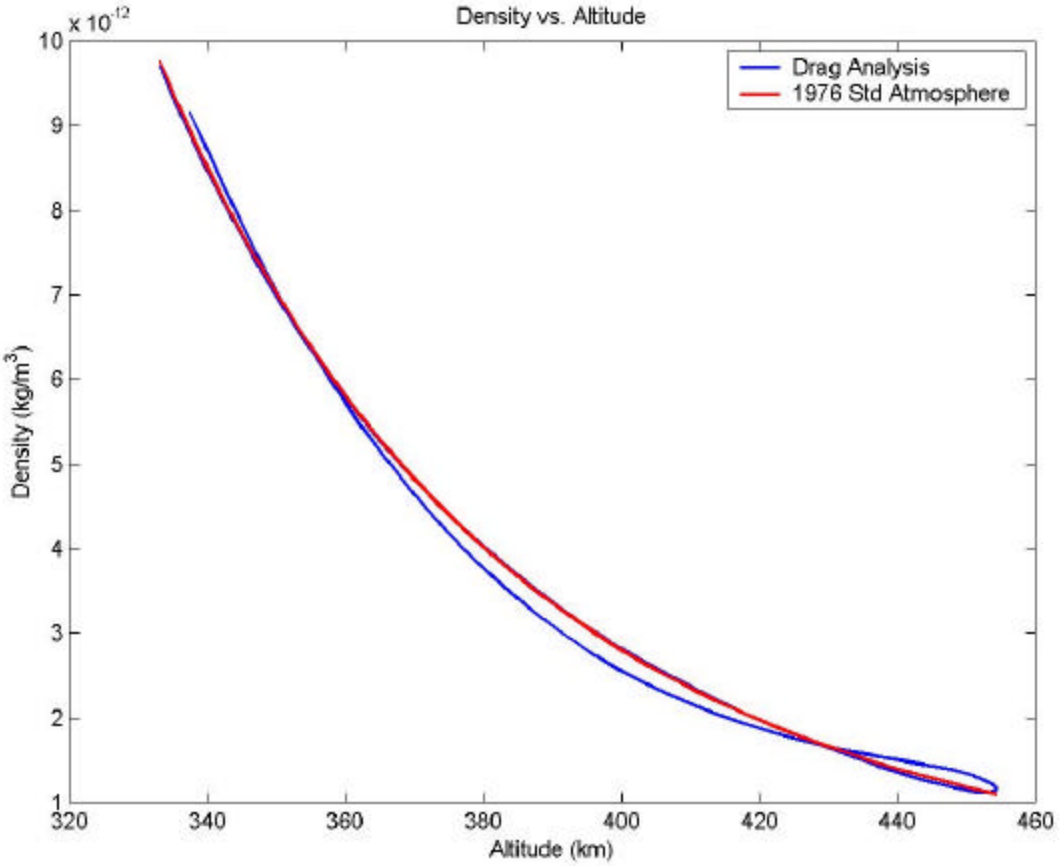

Figure B.35 Density vs. Altitude For an Orbit Defined By:
a = 6778 km
e = 0.01
i = 45°

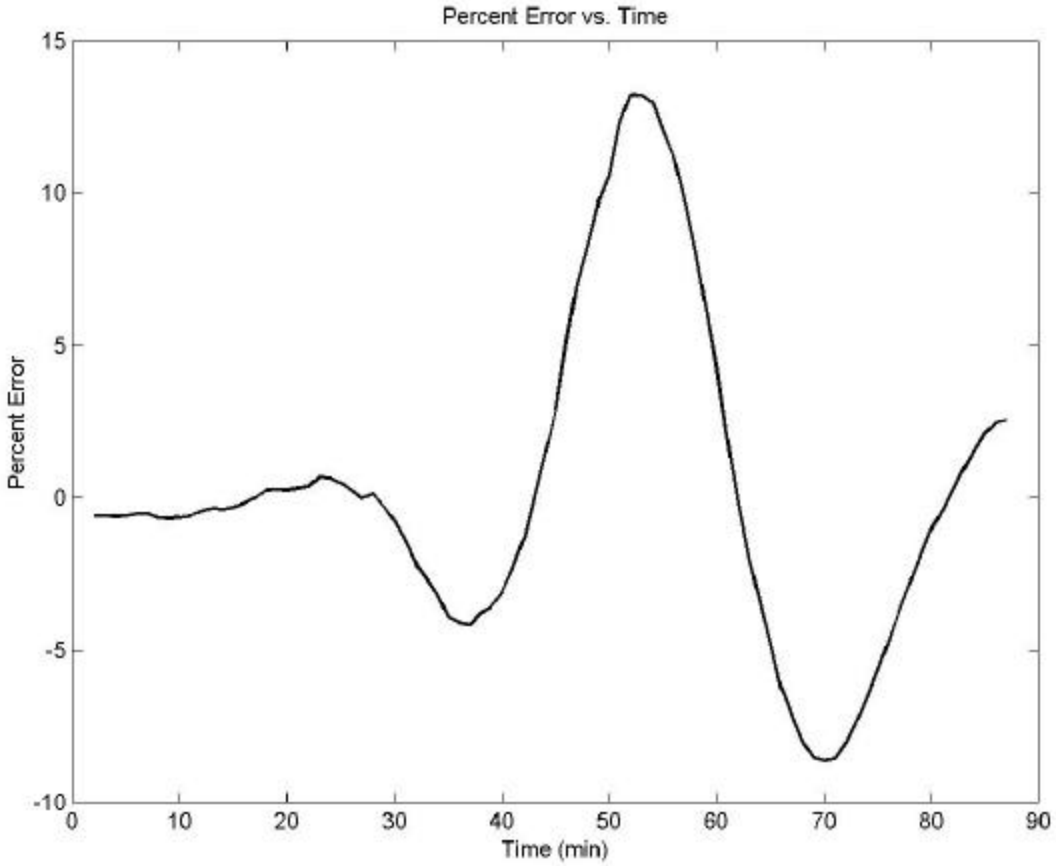

Figure B.36 Percent Error vs. Time For an Orbit Defined By:
a = 6778 km
e = 0.01
i = 45°

Appendix D: Gaussian Variation of Parameters

Vallado[1] derives equation (7) from the Gaussian form of Lagrange's Variation of Parameters. The Gaussian form defines the changes in the classical orbital elements as a function of disturbing forces. The equations are defined in terms of F_R and F_S, the components of a force F. These components are in the RSW coordinate system. The R axis points in the radial direction. The S axis is in the orbital plane and is perpendicular to the R axis, pointing in the direction of motion. The W axis is perpendicular to both the R and S axes, creating a right hand coordinate system.

$$\frac{da}{dt} = \frac{2e*\sin(\nu)}{n\sqrt{1-e^2}} F_R + \frac{2*p}{n*r\sqrt{1-e^2}} F_S \tag{D.1}$$

The flight path angle can be used to divide the force due to drag into components in the RSW coordinate system as seen in equations (D.2) and (D.3).

$$F_R = -\frac{1}{2} \rho \frac{C_D*A}{m} v_{rel}^2 * \sin(\phi_{fpa}) \tag{D.2}$$

$$F_S = -\frac{1}{2} \rho \frac{C_D*A}{m} v_{rel}^2 * \cos(\phi_{fpa}) \tag{D.3}$$

The flight path angle is defined as the angle between the velocity vector and the local horizon. The sine and cosine of the flight path angle can be written as a function of the eccentricity and true anomaly as seen in equations (D.4) and (D.5).

$$\sin(\phi_{fpa}) = \frac{e*\sin(\nu)}{\sqrt{1+2*e*\cos(\nu)}} \tag{D.4}$$

$$\cos(\phi_{fpa}) = \frac{1+e*\cos(\nu)}{\sqrt{1+2*e*\cos(\nu)}} \tag{D.5}$$

Substituting equations (D.2) and (D.3) into equation (D.1), Vallado obtains:

$$\frac{da}{dt} = \frac{2e*\sin(\nu)}{n\sqrt{1-e^2}} \left(-\frac{1}{2} \rho \frac{C_D*A}{m} v_{rel}^2 \right) * \sin(\phi_{fpa}) + \frac{2*p}{n*r\sqrt{1-e^2}} \left(-\frac{1}{2} \rho \frac{C_D*A}{m} v_{rel}^2 \right) * \cos(\phi_{fpa}) \tag{D.6}$$

By reducing equation (D.6), Vallado obtains equation (D.7)

$$\frac{da}{dt} = -\rho \frac{C_D*A}{m} v_{rel}^2 \left(\frac{1}{n\sqrt{1-e^2}} \right) \left[\frac{(e*\sin(\nu))^2}{\sqrt{1+e^2+2*e*\cos(\nu)}} + \frac{p(1+e*\cos(\nu))}{r\sqrt{1+e^2+2*e*\cos(\nu)}} \right] \tag{D.7}$$

Further simplification yields:

$$\frac{da}{dt} = -\rho \frac{C_D * A}{m} v_{rel}^2 \left(\frac{\sqrt{1+e^2+2*e*\cos(\nu)}}{n\sqrt{1-e^2}} \right) \left[\frac{(e*\sin(\nu))^2 + (1+e*\cos(\nu))^2}{1+e^2+2*e*\cos(\nu)} \right] \quad \text{(D.8)}$$

Finally, equation (D.8) can be reduced to obtain:

$$\frac{da}{dt} = -\rho \frac{C_D * A}{m} v_{rel}^2 \left(\frac{\sqrt{1+e^2+2*e*\cos(\nu)}}{n\sqrt{1-e^2}} \right) \quad \text{(D.9)}$$

---

[1] David A. Vallado, Fundamentals of Astrodynamics and Applications, New York: The McGraw Hill Companies, 1997, 559-568, 604-605.

Appendix E: Modeling Atmospheric Rotation

King-Hele[1] derives a scalar equation for calculating the relative velocity of a satellite with respect to the atmosphere. The assumption made in this derivation is that the atmosphere rotates with the Earth.

King-Hele begins with the vector form for the relative velocity of the satellite with respect to the atmosphere where $\vec{v}_{rel}$ is the relative velocity, $\vec{v}$ is the inertial velocity of the satellite, and $\vec{V}_A$ is the inertial velocity of the atmosphere:

$$\vec{v}_{rel} = \vec{v} - \vec{V}_A \tag{E.1}$$

By using the law of cosines, the scalar values can be used to find v_{rel}^2 where g is the angle between $\vec{v}$ and $\vec{V}_A$.

$$v_{rel}^2 = v^2 + V_A^2 - 2*v*V_A*\cos(g) \tag{E.2}$$

Assuming the atmosphere rotates with the Earth, $\vec{V}_A$ can be written as equation (E.3) where r is the magnitude of the satellite's position vector, $\Omega_\oplus$ is the angular velocity of the Earth, and f_{SAT} is the latitude of the satellite.

$$V_A = r*\Omega_\oplus*\cos(f_{SAT}) \tag{E.3}$$

Substituting equation (E.3) into equation (E.2) yields:

$$v_{rel}^2 = v^2 + r^2*{\Omega_\oplus}^2*\cos^2(f_{SAT}) - 2*v*r*\Omega_\oplus*\cos(f_{SAT})*\cos(g) \tag{E.4}$$

Using relationships between a spherical triangle formed by the inclination, latitude of the satellite, and the angle between the velocity vectors results in the following:

$$\cos(i) = \cos(f_{SAT})*\cos(g) \tag{E.5}$$

The resulting equation in terms of the inclination and the satellite's latitude can be written as:

$$v_{rel}^2 = v^2\left(1 - \frac{r*\Omega_\oplus}{v}\cos(i)\right)^2 + r^2*{\Omega_\oplus}^2*\left(\cos^2(f_{SAT}) - \cos^2(i)\right) \tag{E.6}$$

---

[1] Desmond King-Hele, Satellite Orbits in an Atmosphere: Theory and Applications, London, England: Blackie and Son, Ltd, 1987, 29-30.

Bibliography

Bate, Roger R., Donald D. Mueller, and Jerry E. White, Fundamentals of Astrodynamics. New York: Dover, 1971.

Bruinsma, S.L., P. Exertier, R. Biancale, "An Assessment of New Satellite Total Density Data for Improving Upper Atmosphere Models." Planetary and Space Science, 47, 1999.

CIRA 1965: COSPAR International Reference Atmosphere 1965. Amsterdam: North Holland Publishing Company, 1965.

King-Hele, Desmond, Satellite Orbits in an Atmosphere: Theory and Applications. London, England: Blackie and Son, Ltd, 1987.

Marcos, F.A. et al, "Precision Low Earth Orbit Determination Using Atmospheric Density Calibration." The Journal of the Astronautical Sciences, Vol. 46, No. 4, October-December 1998.

Magellan Corporation, Ashtech G-12 HDMA GPS Board Information.

MATLAB® Ver 5.3, The Mathworks, Inc. 1999.

Vallado, David A, Fundamentals of Astrodynamics and Applications, New York: The McGraw Hill Companies, 1997.

Roemer, M, "Recent improvements in our knowledge of neutral atmosphere structures from satellite drag measurements." Radio Science, February 1974, vol. 9. no. 2.

Satellite Tool Kit® Ver 4.1.1b, Analytical Graphics Inc. 2000.